Effects of Modulus of Elasticity of Collagen Sponges on Their Cell-Mediated Contraction In Vitro

by

Donna Schulz Torres

B.S., Mechanical Engineering (1995)
Southern Illinois University at Carbondale

Submitted to the Department of Mechanical Engineering
in partial fulfillment of the requirements for the degree of

Master of Science

at the

MASSACHUSETTS INSTITUTE OF TECHNOLOGY

June 1998

Author .....
Department of Mechanical Engineering
May 8, 1998

Certified by .....
Myron Spector
Senior Lecturer, Department of Mechanical Engineering
Thesis Supervisor

Accepted by .....
Ain A. Sonin
Department of Mechanical Engineering
Chairman, Graduate Thesis Committee

Effects of Modulus of Elasticity of Collagen Sponges on Their Cell-Mediated Contraction In Vitro

by

Donna Schulz Torres

Submitted to the Department of Mechanical Engineering
on May 8, 1998, in partial fulfillment of the
requirements for the degree of
Master of Science

Abstract

Highly porous collagen-glycosaminoglycan (CG) sponges, ultimately to be used as cell-seeded implants to facilitate the regeneration of selected soft tissues, were synthesized and cross-linked to various degrees using both chemical (ethanol, glutaraldehyde) and physical (dehydrothermal, ultraviolet irradiation) methods. Tendon fibroblasts were seeded into the scaffolds and the contraction of the sponges evaluated at 3, 7, 14, and 21 days post-seeding. The cell-mediated contraction of the sponges was calculated as the difference between contraction of the seeded sponges and unseeded control scaffolds exposed to the same *in vitro* conditions, normalized by the DNA content of the sponges. The cell-mediated contraction for each cross-link group was then plotted against the modulus of elasticity for that group, as determined by mechanical testing. Immunohistochemistry using a monoclonal antibody to α-smooth muscle actin was performed to determine if the contractile actin isoform was associated with the cell contraction of the sponges.

Linear regression analysis showed a trend of decreasing cell-mediated contraction with increasing modulus of elasticity, and that dehydrothermal (DHT) treatment of CG sponges alone is not sufficient to resist contraction by seeded tendon fibroblasts *in vitro*. Cross-linking of collagen sponges so that their elastic moduli is at least three times that of sponges cross-linked by DHT alone may be necessary to sufficiently improve their contraction resistance.

Alpha-smooth muscle actin was seen in the cytoplasm of most cells in all sponges at all time periods. This ubiquitous presence of myofibroblasts suggests that these specialized contractile cells are responsible for the contraction of the CG sponges.

Thesis Supervisor: Myron Spector
Title: Senior Lecturer, Department of Mechanical Engineering

Acknowledgments

I would like to thank Professor Myron Spector for your tremendous support, guidance, and enthusiasm. Thank you for believing that mechanical engineers *can* culture cells, and for giving me the chance to work on a project from which I learned so much.

I would also like to express my gratitude to Professor Yannas for the opportunity to work in your laboratory and to learn from you.

Thank you Toby, for all of your hard work. A big part of this thesis would not have been possible without your assistance and I am truly grateful for your help. I must also thank Professor Gibson for the use of her equipment and laboratory facilities.

Many thanks to Sandra for teaching me so much about histology, and for helping me finish on time by sectioning *all* of those paraffin blocks.

Thanks to Martha – you helped me out when I really needed it, and your contagious enthusiasm for your research helped to refuel my own.

To Libby – although you were busy trying to finish your work, you took the time to help me get started on my project. Thanks, and sorry about any cells I killed.

To Mark and Lila – thanks for all of the support and friendship and for pushing me to finish this on time (well, sort of). I *am* going to graduate!

Many thanks to Dr. Hsu for getting me started by performing the tendon harvests, to Gretchen for performing DNA assays on about a million specimens, and to Howie, Stefan, Sonya, Karen, Pam, Patricia, Leslie, and Joyi for your various contributions.

Most importantly, I must thank my family: Xavier, thanks for entertaining yourself for so many hours, and for not learning to crawl until after I finished writing. Wade, there is no way for me to thank you enough for all of the sacrifices, support, ideas, help and love that you've given me. I could not have completed this without you.

This material is based upon work supported under a National Science Foundation Graduate Fellowship. Any opinions, findings, conclusions or recommendations expressed in this publication are those of the author and do not necessarily reflect the views of the National Science Foundation.

Contents

List of Figures

List of Tables

Chapter 1

Introduction

1.1 Purpose of Research

Porous collagen sponges of varying composition and architecture have been researched as scaffolds for regeneration of a variety of tissues including bone [44], esophagus [42], skin [5], dura mater [41], and muscle [55]. One specific form of collagen scaffold, a collagen-glycosaminoglycan (GAG) copolymer, serving as an analog of extracellular matrix, has been used successfully as an implant for the regeneration of dermis [7, 50, 58] and peripheral nerve [9, 11]. Promising results have been reported for treatment of defects in the knee meniscus [51], articular cartilage [6], and tendon [37]. For cases in which the scaffold alone may not be sufficient to induce regeneration of tissue, exogenous cells have been seeded into the sponges prior to implantation to aid in the production of new tissue. The addition of some types of cells, however, has been shown to cause contraction of type-I collagen sponges *in vitro* [37, 43]. Shrinkage of the sponges can become problematic in that it changes the shape and size of the implant and its pores. Alterations in the pore diameter may make migration of cells from the surrounding tissue into the scaffolds impossible. Changes in the size and shape of the sponges can make them difficult to implant and when persisting *in vivo*, separate the sponge from surrounding host tissue. The cell-mediated shrinkage of unseeded implants, with the attendant problems noted above, may also occur soon after implantation as endogenous cells infiltrate the sponge and express a contractile

cell phenotype. This thesis addresses the contraction of collagen-GAG sponges by exogenous cells *in vitro*, and to determine suitable methods for controlling the cell-mediated distortion of these scaffolds by altering the modulus of elasticity through cross-linking treatments.

1.2 Background

1.2.1 Regeneration Scaffolds

Investigators have sought to determine methods to treat wounds to favor their regeneration rather than "repair," the end result of which is scar formation. Scar in tissues which have collagen as a primary component of its extracellular matrix (ECM) is characterized by collagen fibers which are aligned differently than in normal tissue. Studies have shown that "functional orientation of the scar tissue matrix components is generally poor and can take years to realign" [24, 58]. In skin, this alternate alignment of collagen fibers can result in tissue which has reduced elasticity and a cosmetically unacceptable appearance.

One promising approach to prevent scar formation has been to implant a porous material to serve as a scaffold for tissue regeneration. By providing a guide, the direction of cell migration and cell alignment can be altered, and as a result, the orientation of the extracellular matrix that they produce can be controlled [20]. It is believed that this "contact guidance" will improve or speed the process of regaining normal orientation and in turn, attaining normal or close-to-normal physiological function of regenerated tissue. Moreover, cell-implant interactions may affect proliferation and matrix synthesis in a way that favors regeneration. A number of materials, both natural and synthetic, have been investigated as regeneration scaffolds in different configurations. Polylactic acid fibers [17], polylactic-polyglycolic acid meshes, and dimethyltrimethylene carbonate-trimethylene carbonate fibers [48] are examples of synthetic materials studied for regeneration of body tissues. Natural materials including collagen fibers [35], carbon fibers [1] , and collagen sponges [7, 9, 11, 37, 50, 51, 58] have also been

researched as aids to facilitate healing of several tissues.

Implantation of scaffolds in various tissues has highlighted the difference in the regeneration capacity between highly cellular and well-vascularized tissues such as dermis, and avascular or poorly vascularized tissues with low cell density, such as articular cartilage, ligament and tendon. In these latter tissues, scaffolds alone do not appear to be able to induce regeneration. This finding has caused researchers to investigate the use of scaffolds for transplanting exogenous cells to a wound site, as well as for providing contact guidance for regrowth of tissue. To this end, investigators have researched the behavior of various cell types seeded onto synthetic [8, 54], and natural [18] polymers to be used for transplanting dermal fibroblasts [19], chondrocytes [21], and tendon fibroblasts [56] into tissues.

Collagen-Glycosaminoglycan Sponges. The porous collagen-GAG (CG) graft copolymer sponge used in this study has been used successfully in regeneration of dermis and peripheral nerve [25]. In full-thickness dermal wounds, CG sponge sheets with randomly oriented pores acted as a substrate over which dermal fibroblasts could migrate and begin to regenerate dermis [58, 59]. In the peripheral nerve, cylindrical sponges with uniaxial pore channels served as guides for regrowth of axons in a transected nerve [9, 11]. CG sponges were also investigated as implants to regenerate tendon following full transection of the Achilles tendon in a rabbit model [38]. In this case, the CG sponge arrested the development of tendon scar, but the newly formed tissue did not have the fiber orientation, crimp, and strength of normal tendon at 12 weeks post-implantation. This finding prompted investigators to consider seeding the CG sponges with tenocytes [36]. Earlier work investigated the addition, *in vitro*, of keratinocytes onto the CG matrices used for dermal regeneration to produce a one-stage implant for skin regeneration [45]. More recent studies have focused on seeding the CG sponges with chondrocytes from articular cartilage [43] onto CG sponges of varying shape and pore size.

Although the CG sponge has been used primarily without the addition of exogenous cells prior to implantation, the porous architecture which encourages cell migration from host tissue also makes the CG sponges suitable candidates for cell-seeding.

Preliminary studies have shown that seeded cells from various tissues can attach to and proliferate within these sponges *in vitro* [36, 43]. These factors, combined with the desire of researchers to develop cell-seeded CG sponge implants, prompted the use of the CG sponges for this thesis.

1.2.2 Fibroblasts and Myofibroblasts

Fibroblasts are the predominant cell type in many connective tissues including dermis, tendon, and ligament. Fibroblasts are responsible for the maintenance of these tissues through degradation and formation of the collagen extracellular matrix. During wound healing, fibroblasts migrate into the wound bed, and according to some researchers [23], provide the force needed for wound closure through their migration. In this theory of wound contraction, the movement of fibroblasts act as "individual units," contracting the granulation tissue in the wound during their migration. Others have credited wound contraction to a special type of cell which has features of both smooth muscle cells and fibroblasts. These cells were first called "myofibroblasts" in 1971 [31], when Gabbiani, *et al.* noted several ultrastructural features that distinguished these cells from normal fibroblasts, including "cytoplasmic longitudinal bundles of microfilaments (stress fibers) with scattered dense bodies" [16]. In the transmission electron microscope, myofibroblasts can also be characterized by nuclear folds, basal lamina-like cell surface material, and complex cellular junctions [47]. Cell-to-cell contacts between myofibroblasts are said to be responsible for the formation of a contractile network of myofibroblasts which act in concert to produce wound contraction.

The presence of α-smooth muscle actin, the contractile actin isoform found in smooth muscle cells, also distinguishes myofibroblasts from fibroblasts. Immunohistochemical staining with a monoclonal antibody to α-smooth muscle actin can be used to identify this actin isoform in the cytoplasm of cells [49].

Gabbiani's 1971 work on myofibroblasts focused on the role that these contractile cells played in the granulation tissue of wound healing. Since that work was published, various researchers have investigated the behavior of these specialized cells

both *in vivo* and *in vitro*. The *in vivo* studies have mostly focused on the presence of the myofibroblast in healing wounds in tissues such as dermis [16, 26] , ligament [27], and tendon [46]. In addition, the presence of the myofibroblast in normal, uninjured tissues has also been noted [15, 33], although to a lesser degree than in healing tissues [46].

1.2.3 Fibroblast and Myofibroblast Contraction of Biomaterials

Many studies of fibroblast behavior *in vitro* have dealt with the cells' ability to contract gels and lattices composed of collagen [2, 4, 28] and fibrin [53]. These collagen gels comprised a network of thin collagen fibrils with nominal pore diameters less than 10 μm. These gels were useful for certain investigations *in vitro*, but their properties were not suitable for implants. Fibroblast-populated collagen gels contracted to a small fraction of their original size within days, and the degree and speed of contraction directly correlated with the number of cells in the gel. Gels which were attached to their culture dishes also did not undergo the same degree of contraction as free-floating gels. In addition, fibroblasts in gels which were anchored realigned themselves along the stress patterns of the lattice and reorganized the lattice according to the location of the anchors [3]. Erlich and Rajaratnam questioned whether fibroblasts or myofibroblasts were responsible for contraction of collagen lattices [22]. They described "highly oriented sheets of cells" at the lattice periphery which were "morphologically identifiable as myofibroblasts." It had previously been reported that these cells, which had formed "highly oriented sheets" and had "actin-rich staining cytoplasmic stress fibers" were acting as a contractile network to reorient the collagen fibrils around them. In the interior of the lattice, however, randomly oriented cells with fewer cell-cell contacts and only lightly stained actin filaments were found. Erlich and Rajaratnam described these cells as "single units" which used the forces produced by their migration to contract the lattices. Their contention was that fibroblasts reorganize the collagen fibrils of the lattice during their locomotion, until

the collagen can no longer be organized. At this point, the cell-cell contacts begin to form and myofibroblast morphology becomes apparent. According to this theory, the myofibroblasts are not responsible for the lattice contraction, but instead indicate the end stage of contraction. While these theories of collagen gel contraction have been well researched, the cell mechanism of matrix contraction is still in question.

Contraction of collagen sponges by several cell types has been reported. Louie, et al. noted that tenocytes seeded onto half-cylinders of type I CG sponges contracted them to 50% of their original area after 14 days in culture [36]. In some cases, there was also a distinct curling up of the edges of the sponges [37]. In other work, type I CG sponges seeded with chondrocytes contracted to a greater extent than did type II collagen sponges [43]. In another recent study of bovine knee meniscus cells seeded into type I CG and type II collagen sponges [40], the results were similar to those of the articular chondrocyte study. In each of these cases, it was suggested that a suitable method needs to be found to control, prevent, or otherwise design for this contraction of cell-seeded type I CG sponges to be used as implants. This current investigation is based, in part, on those suggestions, and seeks not only to understand the mechanism of cell-mediated matrix contraction, but also to determine suitable methods for controlling that contraction.

1.2.4 Cross-linking and Mechanical Properties of Collagen Sponges

Cross-linking of collagen-based scaffolds has been shown to affect the strength, biocompatibility, resorption rate, and antigenicity [57] of these biomaterials. Furthermore, the degree to which these properties are affected by cross-linking is dependent upon the method and degree of cross-linking. Chemical cross-linking with glutaraldehyde has been widely used to alter the strength and degradation rate of various collagen-based biomaterials [34, 52]. Degradation of the biomaterial, however, releases the bound glutaraldehyde which, in certain concentrations, is toxic to cells. Researchers have attempted to avoid the problems of cytotoxic chemical cross-

linking agents through use of physical cross-linking methods including dehydrothermal (DHT) treatment and ultraviolet (UV) irradiation. Cross-linking by DHT treatment is achieved through drastic dehydration which forms interchain peptide bonds [60]. UV irradiation is believed to form cross-links between free radicals which are formed during irradiation [14].

Because the CG sponges are not generally used as permanent prostheses, but rather as templates to regenerate tissue, it has generally not been necessary to change the sponges' mechanical properties to match those of the tissue into which they are implanted. The sponges are meant to serve as scaffolds for regeneration and then to degrade over time. The rate of degradation has been controlled by cross-linking the sponges dehydrothermally [60], with glutaraldehyde [52], and with ultraviolet light [6], resulting in altered mechanical properties of the sponges, as well.

In a study analyzing the mechanical properties of the type I CG sponges at the macroscopic, light microscopic, and electron microscopic levels [13], the strain data from each of these levels strongly correlated with the others, leading the author to conclude that "the macroscopic mechanical behavior of the tissue analog can be interpreted as a statistical averaging of the mechanical behavior exhibited at the microscopic level." The macroscopic stress-strain relation of the sponges was determined to be the "typical concave-up shape characteristic of the behaviour of porous materials and soft tissues" [12]. While the shape of the stress-strain curve of collagen sponges cross-linked with glutaraldehyde for 24 hours was similar to DHT cross-linked sponges, the glutaraldehyde cross-linked sponges had a higher modulus of elasticity.

In attempting to control cell contraction of CG sponges, the mechanical strength of the substrate was considered. Cells have been shown to rapidly and greatly contract three-dimensional collagen gels and two-dimensional elastomeric substrates [32] with very low mechanical stiffness. In contrast, cells do not contract very stiff materials, such as polystyrene tissue culture dishes. In both cases, the cells adhere to the substrate and are able to migrate and proliferate. The difference in contractability, therefore, would appear to be a result of the extreme difference in the stiffness of the materials. This thesis focuses on synthesizing CG sponges of varying stiffness

to test the ability of seeded cells to contract them. The methods used previously to control degradation of the sponges have also been shown to affect their mechanical properties, and these methods have been used for this thesis to produce collagen sponges of varying stiffnesses.

1.3 Specific Aims and Design of Experiments

The primary goal of this thesis is to determine the effect of the modulus of elasticity of collagen sponges on the ability of a specific cell type to contract these sponges *in vitro*. CG matrices with a range of moduli of elasticity were prepared and their contraction by tendon fibroblasts determined *in vitro*. Tensile tests were performed on sponges which had been cross-linked to various degrees using chemical and physical cross-linking methods. We sought to determine the modulus of elasticity above which would resist contraction by a particular cell type and cell density. Moreover, we hypothesize that the tendon cells contracting the CG matrix express the phenotype of myofibroblasts.

1.3.1 CG Sponges

Type I CG copolymer sponges were manufactured for use in this study. *In vitro* cell-mediated contraction has been documented in these particular sponges. The mechanical properties of the CG sponges was controlled by cross-linking the sponges dehydrothermally, with glutaraldehyde [52] and ultraviolet light [6, 40]. It was also concluded that soaking the collagen sponges in 70% ethanol may provide some degree of cross-linking and protection from shrinkage and degradation, and therefore the study included one group that was treated in this manner. Type II collagen-GAG sponges [43] which were shown to resist contraction when seeded with chondrocytes were also used in this study for comparison with the type I CG sponges.

1.3.2 Cell-Seeding and Measurement of Contraction

Fibroblasts were harvested from calf tendon and seeded onto the type I CG sponges of various stiffnesses and onto type II collagen sponges. The cell-seeded sponges remained in culture for 3, 7, 14, and 21 days. The size of the sponges was recorded prior to seeding and again following their sacrifice from culture in order to quantify contraction.

Histological analysis of cell infiltration, cell morphology, and pore contraction was performed using the light microscope. Immunohistochemical staining of the sponges was done to verify the presence of myofibroblasts.

1.3.3 Mechanical Testing of CG Sponges

Tensile tests were performed on the CG sponges in order to determine the macroscopic stress-strain behavior of CG sponges cross-linked by various methods and to various degrees. Sponges from each cross-link group were strained at a constant rate until failure. The strain was measured and engineering stress computed.

Chapter 2

Materials and Methods

2.1 Fabrication of Collagen Sponges

2.1.1 Type I Collagen-Glycosaminoglycan

CG Slurry Production. The manufacture of the type I CG sponges followed a previously published protocol [10]. Dry, microfibrillar type I bovine tendon collagen was obtained from Integra LifeSciences, Plainsboro, NJ, and stored at 4°C. The slurry was prepared by blending 3.6 g of the collagen with 600 ml 0.05 M acetic acid in a jacket-cooled blender (Eberbach Waring restaurant model blender, Ann Arbor, MI) at 4°C and approximately 23,000 rpm. Following 90 minutes of blending, 120 ml of chondroitin-6-sulfate (chondroitin sulfate C, Sigma Chemical, St. Louis, MO) solution (0.11% w/v) was added to the collagen solution while blending over 15 minutes, using a peristaltic pump. The collagen-chondroitin-6-sulfate coprecipitate suspension was blended for another 90 minutes following the addition of the chondroitin sulfate.

The CG slurry was then degassed by applying a vacuum to a 6 liter sidearm flask containing the slurry for ten minutes. Slurry that was not used immediately was stored at 4°C for no longer than one month. If the slurry was stored for more than one week, it was re-blended on low speed for 10 minutes and degassed before use.

Lyophilization of CG Slurry. Freeze-dryer trays were divided into three sections, each 320 mm × 490 mm. Two hundred twenty-five ml of the CG slurry was pipetted

into each section of the freeze-dryer trays with special care taken to avoid formation of air bubbles. The trays were placed in the freeze-dryer chamber (Virtis Genesis Freeze-Dryer, model 25LE, Virtis, Inc., Gardiner, NY) the temperature of which had been lowered to $-45°C$. The slurry was allowed to freeze for a minimum of one hour before the vacuum pressure was decreased to 200 mtorr or below, and the temperature of the chamber raised to 0°C. Following 12 hours of sublimation, the chamber temperature was raised to 20°C. The freeze-dried slurry, now in the form of a porous collagen sponge, was allowed to dry at 20°C for 90-120 minutes.

2.1.2 Type II Collagen

The type II collagen sponges used in this study were provided by Geistlich Biomaterials. The sponges (Chondrocell-A, batch no. 914106, Geistlich Biomaterials, Wolhusen, Switzerland) were reconstituted from porcine cartilage and packaged sterilely as 2 cm $\times$ 2 cm square sponges which were 5-6 mm thick, and were uncrosslinked. The sponges were determined to have an average pore diameter of 297 μm and a GAG content of approximately 2.0% [6]. The production protocol for Chondrocell is proprietary information of Geistlich Biomaterials and has not been published.

2.2 Cross-Linking of Collagen Sponges

2.2.1 Dehydrothermal Cross-Linking

The 2-3 mm thick sponges were removed from the freeze drier trays and placed in aluminum foil packets. The foil packets were placed in a vacuum oven (Fisher Isotemp vacuum oven, model 201, Fisher Scientific, Medford, MA) at 105°C and 30 mtorr for 24 hours for dehydrothermal(DHT) cross-linking. The sponges were stored in a dessicator at room temperature. All type I CG sponges were DHT cross-linked prior to any additional chemical or physical cross-linking.

2.2.2 Ultraviolet Light Cross-Linking

Type I and type II collagen sponges were cross-linked under ultraviolet (UV) light in a sterile vertical flow hood. The sponges were placed 30 cm from an ultraviolet lamp (Philips Sterilamp #G10T5 1/2 L, l=253.5 nm) which was rated at 5.3 W total output, 55.5 W/cm^2 at 1 m. Type I sponges were cross-linked for 12 hours, and type II sponges were cross-linked for 16 hours. In each case, the sponges were turned over midway through the cross-linking period to expose each side to the same amount of UV radiation.

2.2.3 Glutaraldehyde Cross-Linking

Type I collagen sponge specimens used for mechanical testing and *in vitro* experiments were cross-linked to varying degrees with glutaraldehyde (25%, Sigma Chemical Co, St. Louis, MO). The specimens were first rehydrated in 0.05 M acetic acid for 24 hours at room temperature. They were then soaked in a 0.25% glutaraldehyde in 0.05 M acetic acid for 30 minutes, 12 hours, or 24 hours. At the end of the cross-linking time period, the specimens were repeatedly and exhaustively rinsed in distilled, deionized water to remove any traces of free glutaraldehyde. The sponges remained in water for 24 hours, and were then stored in phosphate buffered saline (PBS) at 4°C. The solutions for cross-linking and rinsing the sponges for the *in vitro* study were sterilized by autoclave (121°C, 15 lb/in^2, slow exhaust) for 25 minutes or sterile filtered through a .2 μm filter (Zapcap-S, Schleicher & Schuell, Keene, NH). The *in vitro* specimens were stored at 4°C in sterile PBS for no more that 2 days before use.

2.2.4 Ethanol Treatment

The type II sponges which had been UV cross-linked for 16 hours and type I sponges which had not undergone any cross-linking other than DHT treatment were soaked in 70% ethanol for 10 minutes. The sponges were then thoroughly rinsed 3 times with PBS and stored in PBS at 4°C. The different cross-linking and treatment groups are summarized in Table 2.1.

Group	Collagen Type	Cross-linking Treatment
DHT	I	Dehydrothermal (DHT) only
UV	I	DHT, UV light, 12 hours
12G	I	DHT, Glutaraldehyde, 0.25%, 12 hours
24G	I	DHT, Glutaraldehyde, 0.25%, 24 hours
0.5G	I	DHT, Glutaraldehyde, 0.25%, 30 minutes
ETH	I	DHT, 70% ETOH 10 minutes
IIE	II	UV light, 16 hours, 70% ETOH 10 minutes

Table 2.1: Experimental cross-linking groups.

2.3 Mechanical Testing

2.3.1 Specimen Preparation

Type I CG. For each cross-linking or treatment group, three specimens for mechanical testing were cut from the dry CG matrix sheets using a scalpel blade. The specimens were 25 mm × 85 mm, and were taken at least 20 mm away from the edges of the sheets. Two parallel lines, 15 mm apart, were marked on the matrix as shown in Figure 2-1 with black fabric paint (Deka permanent fabric paint, Decart, Inc., Morrisville, VT) and allowed to dry for at least 8 hours before rehydration and cross-linking began. Specimens from the UV group were cross-linked under UV light prior to marking.

Type II Chondrocell. The type II sponges used for this study were supplied by Geistlich Biomaterials as 2 cm × 2 cm squares. The squares were UV cross-linked as described above. The type II sponges were then cut into 10 mm × 20 mm pieces. Parallel lines 5 mm apart were marked with the fabric paint (Figure 2-1). The paint was allowed to dry overnight before the sponges were treated with 70% ethanol and rinsed in PBS.

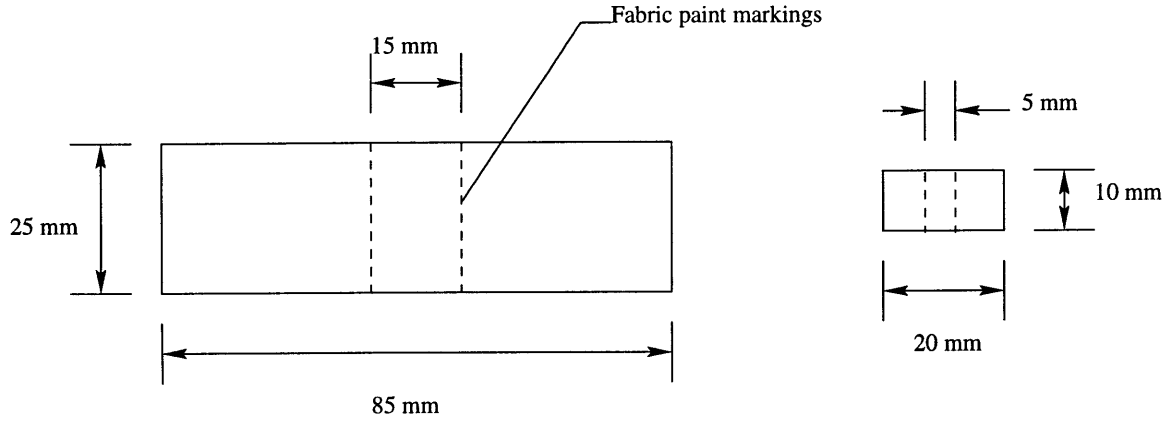

Figure 2-1: Mechanical test specimens.

2.3.2 Testing Procedure

A testing bath was designed [29] to allow a materials testing machine to impart an axial strain on a CG sponge specimen while in 37°C phosphate buffered saline. The acrylic testing bath (Figure 2-2) was clamped onto the base of an Instron materials tester (model 4201, 2.5 N load cell, Instron, Canton, MA). Phosphate buffered saline (PBS) was heated to 37°C and circulated through the bath (VWR Scientific Temperature Bath, model 1104, West Chester, PA). Acrylic clamps were designed to hold the specimen during testing. The clamps were lined with silicone rubber tubing to cushion the specimen, and were tightened with screws.

One end of the marked and hydrated specimens was aligned in one of the acrylic clamps so that the markings faced up and the edges of the sponge were parallel with the edges of the clamp. The clamp was then fixed to one end of the testing bath using a clamp. The free end of the sponge was then placed into the remaining acrylic clamp, with care being taken not to strain the sponge during this process. The sponge remained in the bath for an additional 5 minutes before testing in order to allow it to reach 37°C.

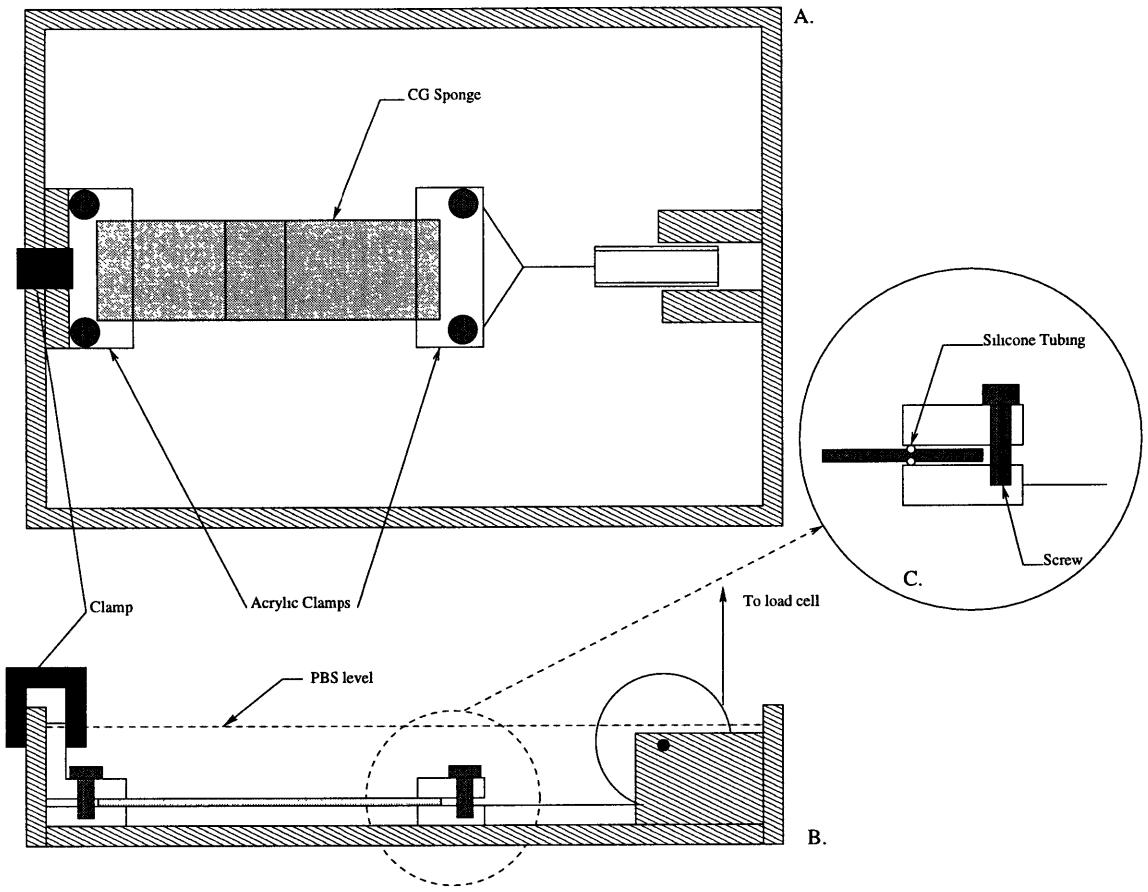

Figure 2-2: Saline bath for mechanical testing. A: Top view of bath. B: Side view of bath. C: Acrylic clamp.

A high-resolution videocamera (Pulnix Progressive Scan High Resolution Videocamera, TM1010, Mountain View, CA) was set up over the testing bath so that the paint lines on the specimen were in focus. The camera image was viewed on a Dell Optiplex GS personal computer using $HLImage++97$. The entire computer screen image was viewed on a Panasonic Pro Line video monitor, along with a running clock generated by a Panasonic date/time generator. A calibration image was recorded by placing a micrometer set to 1 cm at the level of the saline in view of the videocamera.

Once the specimen was in place, the crosshead of the Instron tester was raised until the line connecting it to the free acrylic clamp was almost fully extended but without allowing it to strain the specimen. A second computer (Dell Optiplex GS,

Dell Computer Corp., Round Rock, TX) was used with Labview software to record the load versus time data throughout the test. The date/time generator was triggered as soon as the strain was applied in order to create a time stamp on the videotape of the exact beginning of the test.

Specimens were strained at a rate of 1 mm/min until failure. The entire test was recorded on a Panasonic VCR so that the paint markings were visible on the monitor throughout the test. Two to four specimens were tested for each sponge treatment group.

2.3.3 Data Analysis

For each test, images were captured from the recording at 1 minute intervals. The micrometer calibration image was also caputured. Using $HLImage++97$, three measurements between the paint markings were made for each image. These measurements and the time stamp on the image were recorded and entered into a Microsoft Excel 97 worksheet. The force value recorded at each of the times at which the images were taken was determined based on the time stamp on the image and the force/time data recorded by Labview. The three measurements were averaged and the average strain for each time point was calculated. Because the measurements of strain were given in pixels, these values were compared with the number of pixels measured in the calibration image of a known distance. The engineering stress and strain were computed for each image.

A stress-strain plot was created for each image. A second-order polynomial regression was performed in order to fit a curve to the data. The derivative of the curve equation was taken in order to determine an equation for the modulus of elasticity for each specimen.

2.4 Disk Measurement

2.4.1 Imaging of Disks

For the *in vitro* study, matrix disks 9 mm in diameter were cut from the sheets of CG sponges and the squares of Chondrocell using a punch and hammer under sterile conditions. Following the various cross-linking treatments and immediately prior to seeding, the disks were measured. An overhead projector (3M, Austin, TX) was placed in front of a white screen. A sterile plastic petri dish (Falcon) was filled with sterile cell culture medium and set on the projector so that its image was projected onto the screen. A videocamera (Sony Handycam 8 mm, model CCD-TRV52, Tokyo, Japan) was set on a tripod at a fixed distance from the screen. Once the camera and projector were in place, a dime which had been measured using a micrometer to determine the diameter was placed on the projector and its projected image was recorded on videotape to serve as a reference. Each disk to be seeded was then placed, one at a time, into the PBS filled dish, and its projected image was recorded on videotape. The recorded images of the disks were captured from the videotape using an image capture device (AIGotcha!, AITech, Fremont, CA) and stored as color JPEG images.

2.4.2 MATLAB Analysis of Disk Size

The collagen sponge disks appear in the image as a dark region on a light background. MATLAB code was written to analyze the JPEG images (Appendix A). As each image was read into MATLAB, each pixel had three values associated with it corresponding to the levels of red, blue, and green in the pixel. Using these three values, the "energy" or "brightness" of the pixel was calculated using the following equation:

$$\text{energy} = \sqrt{(\text{red})^2 + (\text{blue})^2 + (\text{green})^2}$$

The pixel energy values were normalized so that the darkest pixel in the image

was given a value of 0, and the brightest pixel in the image was given a value of 1. After normalization, pixels with a value between 0 and 0.5 were classified as "dark", and therefore as being a part of the disk region of the image. Pixels with a value between 0.5 and 1 were considered "light", and classified as being part of the background of the image (Figures 3-12 – 3-13). Because air bubbles and other artifacts floating in the medium also appeared as dark spots on the images, each image was edited using XPaint (written by David Koblas, Mountain View, CA) to erase any extraneous "dark" spots and to prevent them from being counted as part of the sponge area. The algorithm then counts the number of pixels that belong to the disk region, giving an area of the disk in pixels. The area of the disk in pixels was then compared to the area in pixels of the dime which had been imaged and analyzed in the same manner as the disks. This comparison was then used to determine the disk diameter. Each disk was measured in this manner before seeding and following its sacrifice from culture. The sponge disks were numbered according to their cross-linking group and time period, and careful account of each disk was kept so that the pre- and post-seeding diameters of each disk could be compared.

2.5 Fibroblasts

2.5.1 Harvest and Digestion

The patellar tendon was harvested from the knee of a young calf (Research 87, Hopkinton, MA) under sterile conditions. The tendon was placed in sterile D-PBS (Dulbecco's Phosphate Buffered Saline, Life Technologies, Grand Island, NY) with 2% penicillin/streptomycin (5000 U/5000 μg/ml, Life Technologies) and 1% amphotericin B (Fungizone, 250 μg/ml, Life Technologies) and stored at 4°C for no more than 4 hours. The ends of the tendon were removed and any non-tendon tissue was dissected away, leaving only the midsubstance of the tendon. The midsubstance tissue was then dissected into pieces that were approximately 2 mm $\times$ 2 mm. For each gram of tissue to be digested, a 50 ml centrifuge tube was filled with 30 ml of trypsin-

EDTA (0.05% trypsin, 0.53 mM EDTA, Life Technologies). The tubes were attached to a shaker (Labquake shaker, Laboratory and Research Instruments, Berkeley, CA) and agitated at 37°C. After one hour of agitation, the tubes were centrifuged at 1500 rpm for 10 minutes, and the supernatant aspirated. The tissue was throroughly rinsed in PBS, and centrifuged again. The supernatant was removed and 30 ml of a solution of 0.15% collagenase (Type I, Worthington Biochemical Corp., Freehold, NJ) in DMEM/F12 (Life Technologies) was added to the tubes. The tubes were again agitated until digestion was complete, or for a maximum of three hours. The contents of the tubes were then filtered through a 70 μm cell strainer (Falcon, Franklin Lake, NJ). The filtered solution was then centrifuged and aspirated, leaving a pellet of tenocytes. The pellet was twice rinsed in sterile D-PBS and centrifuged in order to remove remaining traces of collagenase. The pellet was resuspended in complete cell culture medium consisting of DMEM/F12, 10% heat inactivated fetal bovine serum (Hyclone Laboratories, Logan, UT), 1% L-glutamine (200 mM, Life Technologies), 1% amphotericin B, 2% penicillin/streptomycin, and ascorbic acid (Life Technologies) at a concentration of 25 μg/ml. The cells were counted with a hemacytometer (Reichert-Jung, VWR Scientific, Boston, MA) using trypan blue (Life Techologies) stain. The cells were then seeded into 75 cm^2 cell culture flasks (Falcon, Franklin Lake, NJ) at a density of approximately 2.5×10^5 cells per flask. Fifteen ml of complete cell culture medium was added to each flask.

2.5.2 Culture and Passage

The fibroblasts were cultured in a humidified chamber at 37°C, and 5% CO_2 (Napco CO_2 Incubator, model 6200, Fisher Scientific, Medford, MA). Culture medium was changed every 2-3 days, and cells were monitored daily for confluence using an inverted phase-contrast light microscope (Nikon, Tokyo, Japan). Spent culture medium was removed from the flasks and replaced with 5 ml of D-PBS. The D-PBS was then removed and 4 ml of trypsin-EDTA was pipetted onto the cell monolayer. After 5-8 minutes in a 37°C incubator, the cells were checked for detachment from the flasks under the inverted microscope, and trypsinized cells were transferred to a

sterile centrifuge tube. An additional 5 ml of complete cell culture medium was used to rinse any remaining cells from the flask and was added to the centrifuge tube. The complete medium also served to stop the trypsinization. The tubes were centrifuged at 1500 rpm for 10 minutes. The supernatant was aspirated and the cells resuspended in 10-40 ml of cell culture medium, depending on the estimated number of cells in the pellet. A cell count was performed with a hemacytometer as described above. The cells were seeded into new flasks at a density of 2.5×10^5 per flask. A portion of the cells from each passage were cryopreserved by adding 5% DMSO (Sigma Chemical, St. Louis, MO) to the cell suspension and storing them in cryostorage vials at $-70°C$.

2.6 Cell Seeding

Preparation for cell seeding of CG and type II sponges began with coating the wells of 12-well culture dishes with a thin layer of sterile 2% agarose (Bio-rad standard low-mr, Bio-rad, Richmond, CA). For each cross-linking group and time period, twelve disks were allocated for seeding, and six served as unseeded controls. Of the seeded disks, 6 were allocated for analysis of DNA content, and the other six were to be used for contraction measurement, histology, and immunohistochemistry. Disks were placed into labeled, agarose coated individual wells filled with complete culture medium prior to measurement as described above. Following the recording of the disks' projected images, the disks were returned to their culture wells and incubated at 37°C while the cells were being prepared for seeding.

Fourth passage patellar tendon fibroblasts were used for the *in vitro* seeding experiment. Cells were trypsinized, centrifuged, and counted as described in section 2.4.2 for passaging. After the cells were counted, the suspension was centrifuged again. The pellet was resuspended so that the cell density was 2.5×10^5 cells per 50 μl. The cell culture medium in the culture wells containing the disks was aspirated. Excess medium was removed from the sponges by placing them on sterile filter paper for 30 seconds. The sponges were then put back in their individual wells. Fifty microliters of cell suspension was pipetted onto each sponge surface. The seeded sponges were

incubated at 37°C for one hour to allow the cells to begin attaching to the surface of the sponge. After the initial hour of incubation, the sponges were turned over, and an additional 50 μl of cell suspension was pipetted onto the unseeded surface, bringing the total number of cells seeded onto each disk to 5.0×10^5. Following another hour of incubation, an additional 3 ml of culture medium was added to each well.

The disks were incubated in an humidified chamber at 37°C and 5% CO_2, with medium changes every 3 days. Specimens were sacrificed from culture at 3, 7, 14, and 21 days post-seeding.

2.7 Histology and Immunohistochemistry

2.7.1 Fixation

Following sacrifice from culture and measurement of the disk size as described above, both the seeded disks and unseeded controls were fixed for histology and immunohistochemistry. Specimens were fixed in 10% neutral buffered formalin (pH 7.4) for 48 hours at 4°C.

2.7.2 Embedding and Sectioning

Paraffin embedding and sectioning. Two of the six seeded specimens and two of the six control specimens allocated for histology were dehydrated through graded ethanol (50%, 70%, 80%, 95%, 95%, 100%, 100%, 100%) in an automatic tissue processor (Tissue-Tek VIP, Miles Laboratory, Mishawaka, IN) to three changes of histoclear (S/P Brand Americlear clearing solvent, Baxter Scientific, Deerfield, IL) for one hour in each solution. The specimens were then infiltrated with three changes of molten paraffin with one hour per change, and then embedded in fresh paraffin. One sponge was embedded flat, and the other was cut in cross-section and embedded with the cut surfaces on the face of the block (Figure 2-3).

Seven micron-thin sections were cut with a microtome (Reichert-Jung Supercut 2050, Leica, Inc., Deerfield, IL) and floated in a 46°C water bath. The sections were

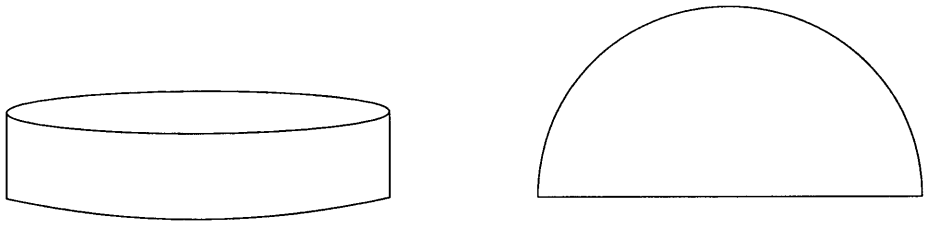

Figure 2-3: Embedding orientation for paraffin and GMA. A: Disk embedded on its flat surface. B: Disk embedded on its cross-section.

picked up on glass slides and dried overnight at 45°C.

Glycolmethacrylate embedding and sectioning. Two seeded and two control specimens were dehydrated through graded ethanol (50%, 70%, 80%, 95%, 95%, 100%, 100%, 100%) and infiltrated with the catalyzed buffer solution A of the GMA embedding kit (JB-4, Polysciences Inc., Warrington, PA). The specimens remained in the infiltrate for 48 hours at 4°C. The sponges were oriented as described above for paraffin sectioning, and polymerized in fresh catalyzed solution A and solution B.

Five micron-thin sections were microtomed and floated onto a room temperature water bath. The sections were collected on glass slides and dried on a warm hot plate for five minutes.

2.7.3 Staining

Hematoxylin and eosin (H&E) staining was performed on both paraffin and GMA sections. The cells stained dark blue, and the collagen sponges stained light pink. For paraffin sections, the slides were twice immersed in xylene for five minutes. The sections were then serially rehydrated through graded ethanol (100%, 100%, 95%, 80%, 70%, two minutes each), and then dipped in Harris' hematoxylin (Sigma Chemical Co., St. Louis, MO) for 10 minutes. Slides were rinsed in tap water for two minutes, and then immersed in acid alcohol (1 ml HCl in 100 ml 70% ethanol) for 2 minutes. The slides were rinsed briefly in tap water, and then dipped in ammonia water (4 drops of ammonium hydroxide in 200 ml distilled water) for two minutes.

Following another two-minute rinse in tap water, the slides were immersed in aqueous eosin Y solution (100 ml distilled water, 100 ml eosin Y, 1 ml glacial acetic acid) for 45 seconds. Slides were rinsed for two minutes in running tap water before serial dehydration (70%, 80%, 95%, 100%, 100% ethanol) and two 5-minute immersions in xylene. After they were completely dried, the slides were mounted (Cytoseal 60, low viscosity, Stephan Scientifics, Riverdale, NJ) and coverslipped.

GMA sections to be stained with H&E were placed directly into Harris' hematoxylin for 90 minutes, and then rinsed for two minutes in tap water. Slides were dipped in acid alcohol for two minutes, followed by a two minute rinse in tap water, and then dipped in ammonia water for two minutes. Following a five minute rinse in tap water, the slides were immersed in eosin Y solution for 5 minutes. The slides were then rinsed for two minutes and allowed to air dry. Slides were mounted and coverslipped as described above for paraffin sections.

GMA sections were also stained with aniline blue to highlight the porous structure of the collagen sponges for image processing. Slides were dipped in 100% ethanol for two minutes, followed by 70% ethanol for two minutes. The slides were then immersed in analine blue (5 g analine blue, 200 ml distilled water, 4 ml glacial acetic acid) for 4 minutes. Two consecutive 1% acetic acid solution rinses (1 minute each) cleared excess aniline blue. The slides were then rinsed in 95% ethanol twice, and in 100% ethanol twice. After air-drying, the slides were mounted (Cytoseal 60, Stephan Scientifics, Riverdale, NJ) and coverslipped.

2.7.4 Immunohistochemistry

Immunohistochemical staining for alpha-smooth muscle actin was performed on 7 μm thin sections of formalin-fixed, paraffin-embedded cell-seeded sponges. The slides were placed in a gently agitated xylene bath for one hour. Following deparaffinization, the slides were rehydrated through graded ethanol (100%, 100%, 95%, 80%, 70%) to distilled water for two minutes in each solution. Slides were rinsed twice in phosphate buffered saline (PBS, cat. #P3813, Sigma Chemical, St. Louis, MO) for two minutes in each rinse. Slides were dried carefully to remove excess

saline while preventing the sections from drying out. A hydrophobic marker (PAP pen, Polysciences Inc., Warrington, PA) was used to circle the sections to be stained. Two drops of a solution of 0.1% trypsin (cat. #T7409, Sigma Chemical) in PBS were placed on the sections and incubated in a humidified chamber at room temperature for one hour. Slides were rinsed twice in PBS (2 minutes per rinse) and dried as described above. Sections were next quenched with 3% hydrogen peroxide (cat. #H1009, Sigma Chemical) for five minutes, and rinsed in PBS. A solution of 20% goat serum (cat.#G9023, Sigma Chemical) was added to the sections and incubated for thirty minutes. Excess goat serum was then removed from the sections, and two-hour incubation with the primary antibody (mouse monoclonal anti-alpha-smooth muscle actin, 1:400 dilution, cat. #A2547, Sigma Chemical), or with the negative control (1% mouse serum, 1:800 dilution, cat. #M5905, Sigma Chemical) began. Slides were again rinsed, with care being taken not to contaminate negative control sections with the primary antibody. The secondary antibody (Goat Anti-Mouse IgG, cat. #B7151, Sigma Chemical) was diluted to 1:200 in PBS, and added to the sections for one hour. Following two rinses in PBS, a 1:50 dilution of ExtrAvidin peroxidase (cat. #E2886, Sigma Chemical) was placed on the sections for 20 minutes. Slides were then rinsed in distilled water, and incubated with AEC chromagen solution (AEC staining kit, cat. #AEC-101, Sigma Chemical), for 10-12 minutes and rinsed again in distilled water. Mayers hematoxylin (cat. #MHS-16, Sigma Chemical) was used to counterstain the sections for twenty minutes, followed by a 20 minute rinse in running tap water. Slides were air-dried, mounted with glycerol gelatin (cat. #GG-1, Sigma Chemical), and coverslipped.

2.7.5 Light Microscopic Analysis

The light microscope (Olympus Vanox AH-2, Olympus America Inc., Lake Success, NY) was used with H&E stained sections to analyze the morphology and density of cells in the sponges. The cells' morphology at the edge and center of the disk (Figure 2-4) was described qualitatively as spheroid (round), ovoid (egg- or oval-shaped), or fusiform (elongated or spindle shaped) based on the shape of the nucleus and es-

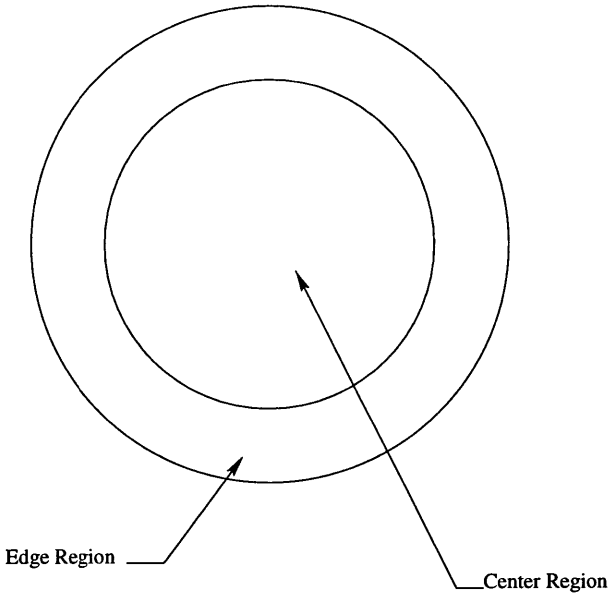

Figure 2-4: Disk regions defined for histological analysis of cell morphology and mean pore diameter.

timating the cell boundaries. Cell morphology in the center and edge regions of the disk were noted. A grid eypiece was used to measure the depth of cell infiltration into the disks in H&E stained cross-sections.

Immunohistochemical staining for alpha-smooth muscle actin was evaluated using the light microscope. The grid eypiece was used to count the percentage of postively stained cells in the two regions of the disk. Five random areas of each region were viewed through the eyepiece, and the postively stained and unstained cells within the grid were counted. This process was repeated on four sections from two specimens for each group analyzed.

The change in pore size of both seeded and control sponges with time was also evaluated qualitatively using the light microscope. The grid eyepiece described above was used to estimate the pore diameters in the edge and center regions for sponges from each treatment group and time period.

2.8 DNA Assay

Six sponges from each treatment group at all time periods were allocated for analysis of DNA content. At sacrifice, sponges were rinsed with PBS and stored at $-70°C$. The sponges were digested in 1 ml of 0.5% papain/buffer solution in a 65°C water bath. A 200 μl aliquot of the digest was combined with 40 μl of Hoechst dye no. 33258 (Polysciences, Inc, Warrenton, PA), and evaluated fluorometrically (Hoefer Scientific Instruments DNA Fluorometer). The results were extrapolated from a standard curve using calf thymus DNA. For one run of the DNA assay, a standard curve based on a sample of tendon cells from the same source as those seeded was used to estimate the cell number from the DNA measurement.

2.9 Statistical Analysis

Results are given as means and standard error of the mean (s.e.m.) unless otherwise noted. For stress-strain data, second-order polynomial regression was performed to determine the stress-strain relation. Linear regression analysis was performed to determine the relationship between cell-mediated sponge contraction and sponge modulus of elasticity. ANOVA and student's t-tests were performed to determine significance between groups. Statistical analysis was performed with Microsoft Excel 97 (Microsoft Corp., Redmond, WA) or Statview (SAS Institute, San Fransisco, CA).

Chapter 3

Results

3.1 CG Sponge Synthesis and Preparation

3.1.1 CG Sponge Synthesis

CG sponges were produced in 2-3 mm thick rectangular sheets. On occasion, the sheets had areas which were much thicker (4-5 mm) or much thinner (1 mm or less) than the rest of the sponge. These areas were not used for mechanical testing or seeding. Qualitative analysis of pore diameters in the sponges revealed pore diameters ranging from 20 μm to 400 μm, with an average of 120 μm. Pores were randomly oriented throughout the sponges. CG sponges with similar pore characteristics were used previously for dermal regeneration studies [25].

3.1.2 Preparation of Sponges for Seeding and Mechanical Testing

Both the disks used for the cell-seeding experiment and the specimens used for the mechanical testing were cut from the sheets of sponges. The mechanical test specimens were cut with a scalpel blade, and no gross distortion or compression of pores by the blade was found. The sponges to be seeded, however, were cut from the sheets using a metal punch and hammer. Although the punch was resharpened

several times throughout the cutting process, the edges of the disk often appeared to be compressed by the punch. The process of rehydration appeared grossly to have restored the normal pore structure at the edges.

Type I CG sponges which were cross-linked with glutaraldehyde for 12 and 24 hours were noticeably stiffer following cross-linking. They also appeared slightly yellow in color when compared to the bright white color of the other groups. The type II collagen sponges became swollen to 1.5 times their original diameter when rehydrated with ethanol and rinsed with saline.

The type II sponges appeared to be structured in a laminar fashion. If not handled very carefully, layers of the sponge could be separated from the rest of the sponge. Slight swelling in the type I CG sponges was apparent only in the glutaraldehyde-treated sponges.

Specimens for mechanical testing were marked with fabric paint to define a gauge length for strain measurements. The paint remained largely intact throughout the various treatments and the tensile tests.

3.2 Mechanical Testing

3.2.1 Type I CG Sponges

Two to four specimens were tested for each type I CG cross-linking group (Table 2.1). At a strain rate of 1 mm/min, tests generally took between 20 and 30 minutes to reach failure. Failure occurred at points in the specimens that were at least 15 mm from the clamped end, with approximately half of the failures occurring within the gauge length, and the other half occuring just outside the gauge length. For each mechanical test of a type I CG sponge, the engineering stress was plotted as a function of the strain. A second order polynomial regression was performed to determine the relationship among the data points. The equation of the curve and the coefficient of determination for each curve are shown on the chart corresponding to the specimen's cross-linking group (Figure 3-1 – Figure 3-6). The p-value for all curves was less

than 0.001. Figure 3-7 compares representative stress-strain curves for each of the treatment groups.

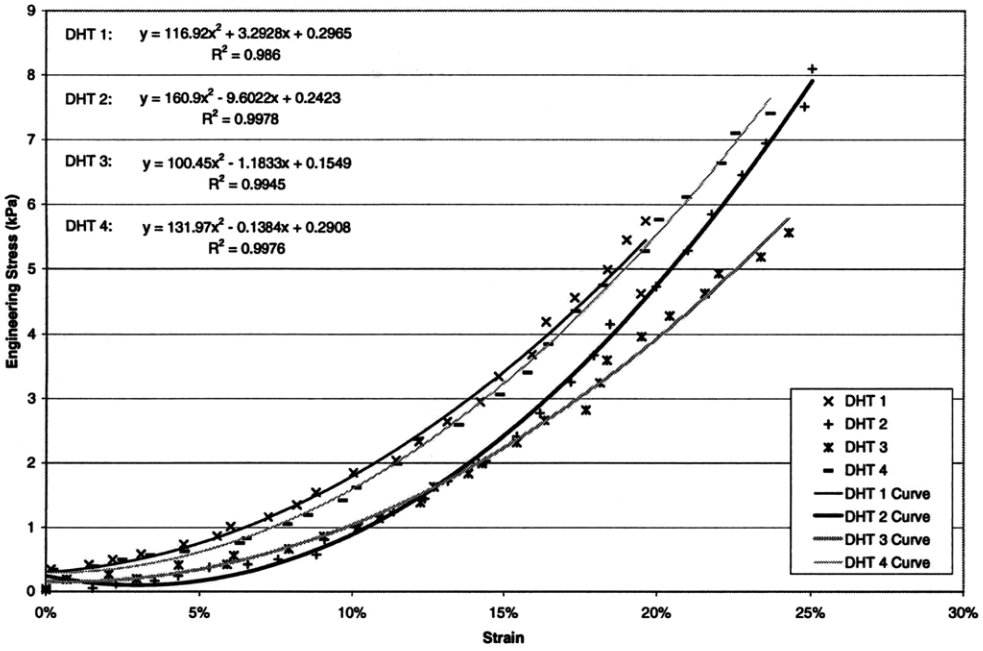

Figure 3-1: Stress-strain behavior of dehydrothermally (DHT) cross-linked type I CG sponges.

The slope of the stress-strain curve is representative of the "apparent modulus of elasticity" of the porous material, reflecting the deformation of the solid substance and the voids. For the purposes of this thesis, this parameter will be referred to as the modulus of elasticity. The equation to determine the modulus of elasticity of the type I CG sponges was determined by taking the first derivative of the second-order polynomial equation of the curve fit to the data points. The modulus values were then calculated at 5, 10, and 15% strain. Moduli for the various groups are compared in Figure 3-8, and summarized in Table 3.1. As expected, the modulus increased with increasing treatment time in glutaraldehyde, and the DHT group had the lowest modulus of all groups. The ethanol, 0.5G, and 12G groups all had similar moduli, while the UV and 24G sponges had the highest moduli of elasticity.

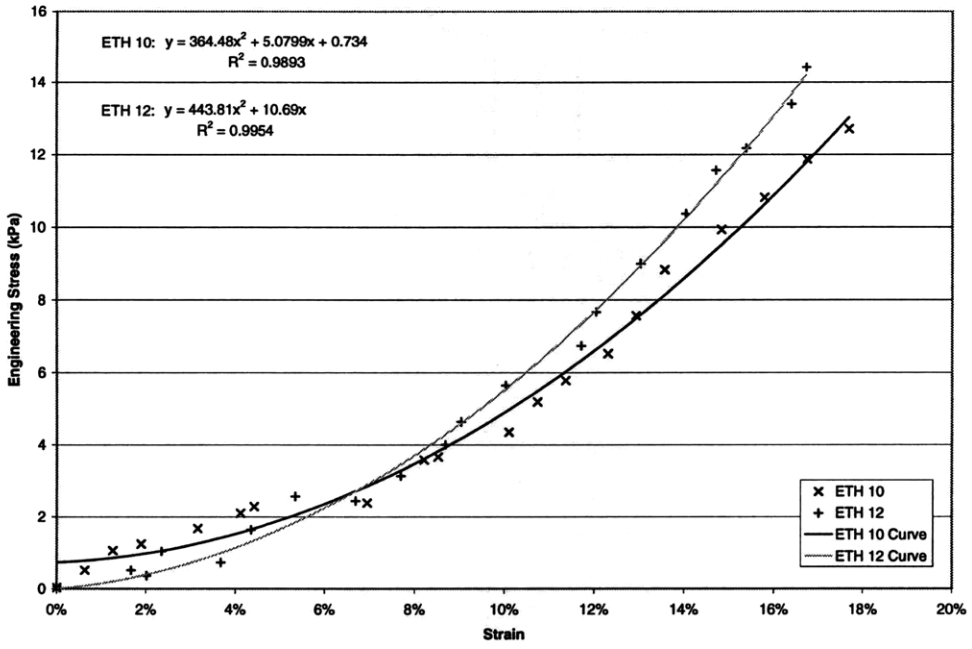

Figure 3-2: Stress-strain behavior of ethanol-treated dehydrothermally cross-linked type I CG sponges.

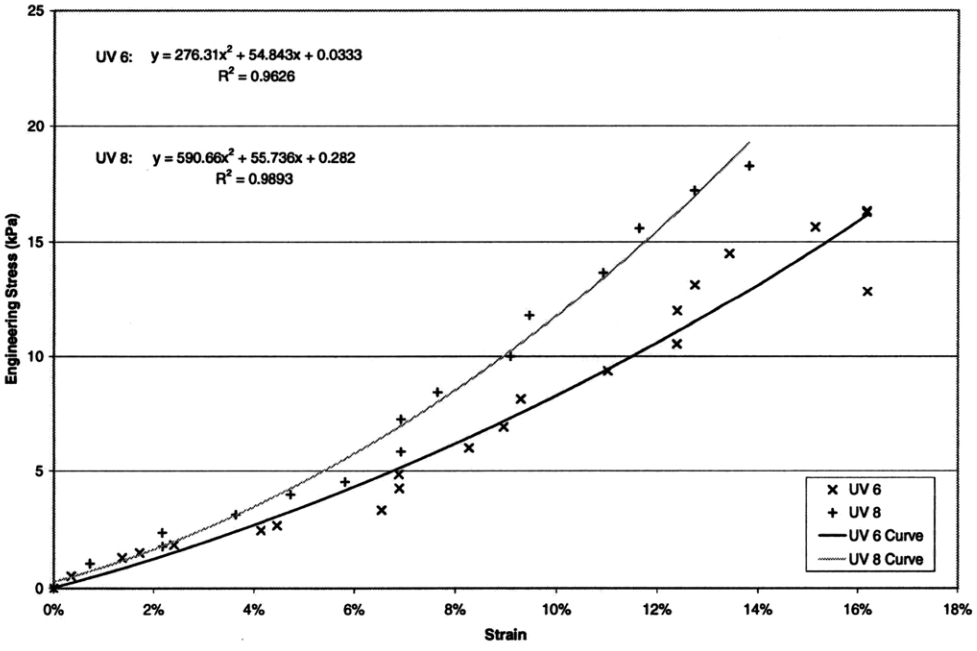

Figure 3-3: Stress–strain behavior of ultraviolet light–irradiated type I CG sponges.

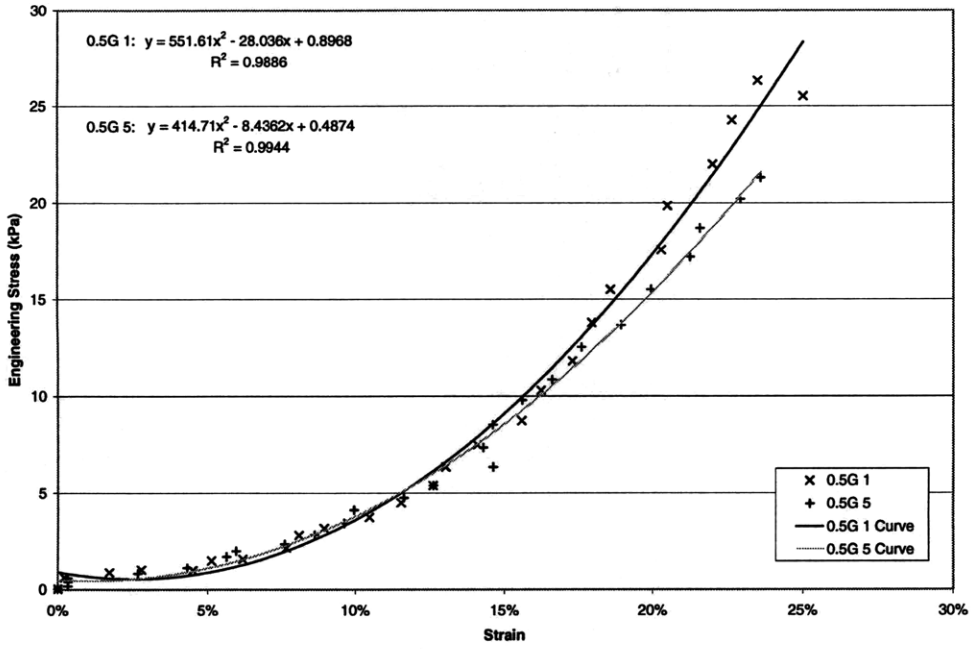

Figure 3-4: Stress-strain behavior of type I CG sponges cross-linked in glutaraldehyde for 30 minutes.

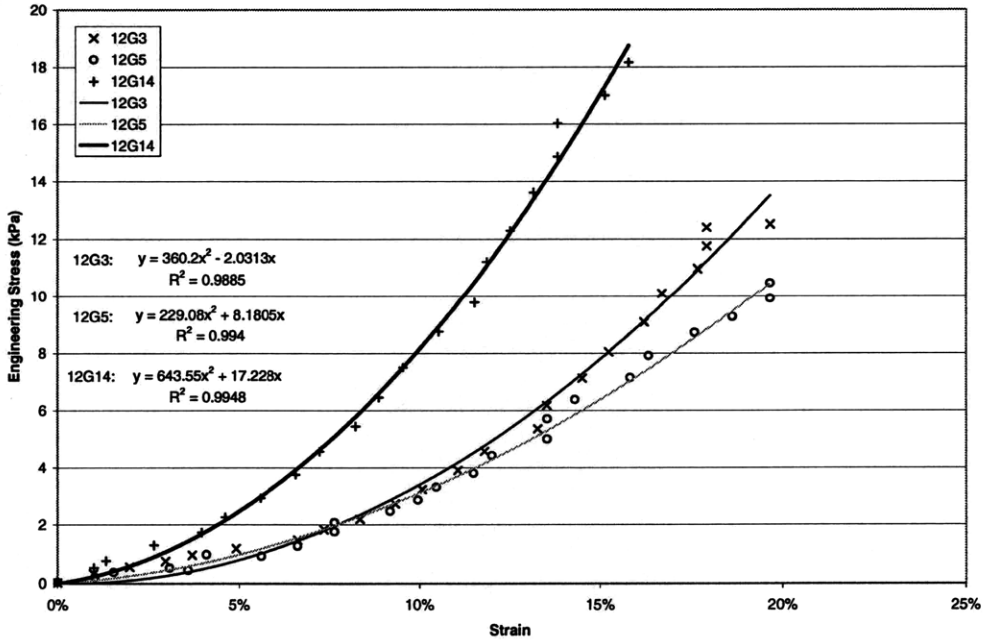

Figure 3-5: Stress-strain behavior of type I CG sponges cross-linked in glutaraldehyde for 12 hours.

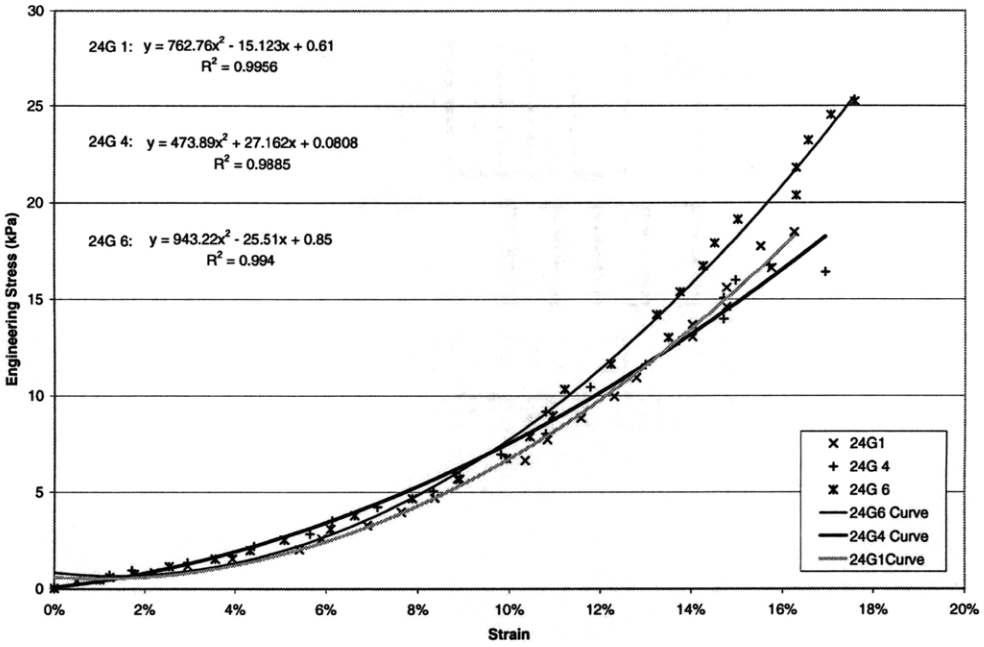

Figure 3-6: Stress-strain behavior of type I CG sponges cross-linked in glutaraldehyde for 24 hours.

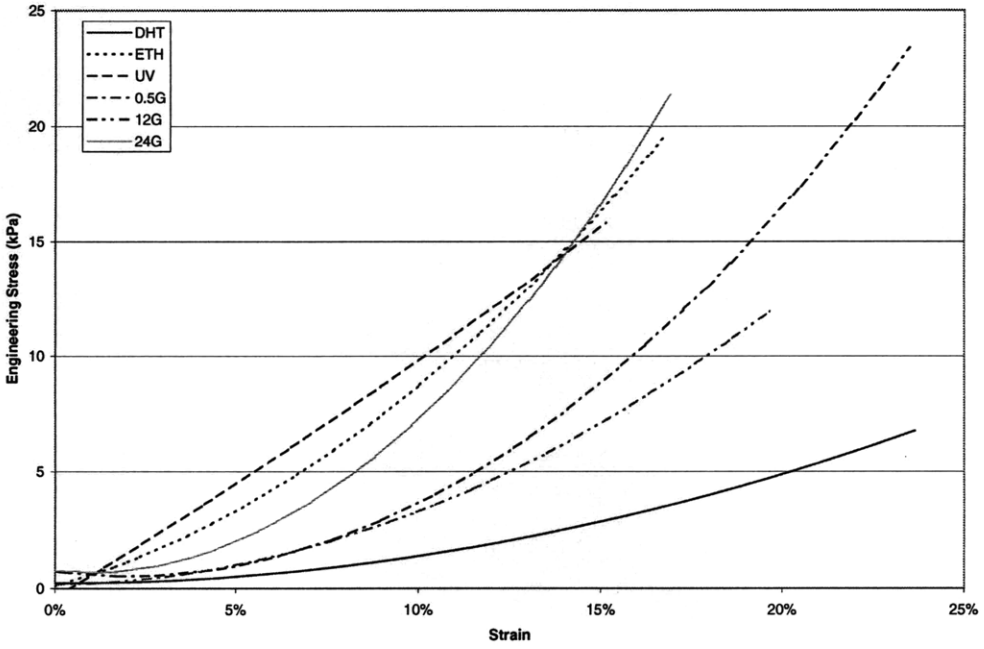

Figure 3-7: Representative curves of stress-strain behavior of type I CG sponges.

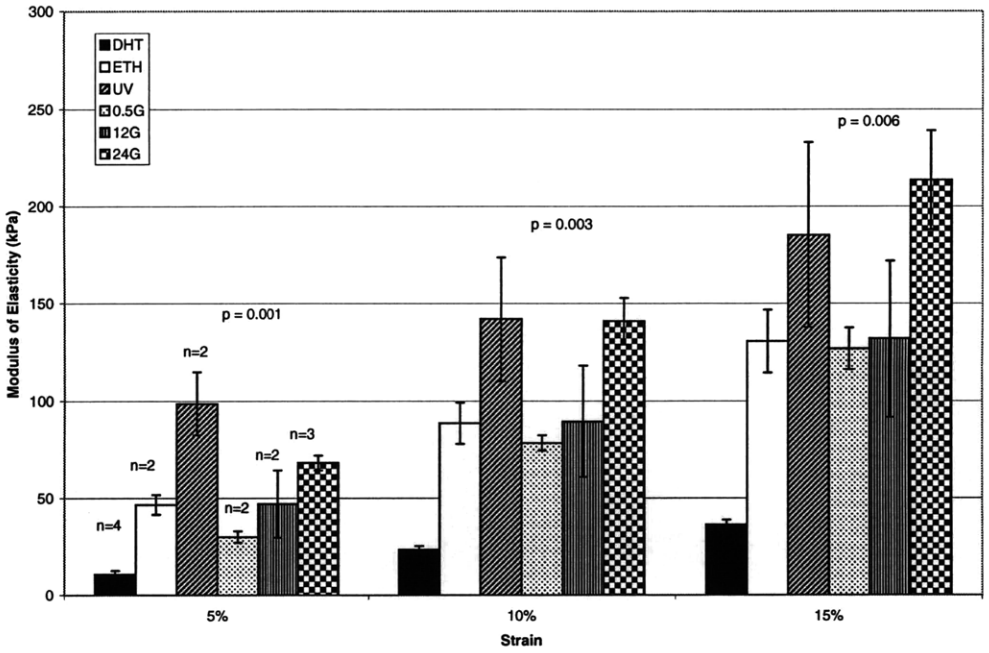

Figure 3-8: Modulus of elasticity of type I CG sponges at various strains. The moduli were derived from the equations for the stress-strain curves. P-values determined by one-way ANOVA (mean $\pm$ s.e.m.).

Group	n	5% Strain	10% Strain	15% Strain
DHT	4	10 ± 1	23 ± 1	36 ± 2
ETH	2	46 ± 5	88 ± 10	130 ± 16
UV	2	98 ± 16	142 ± 31	185 ± 47
0.5G	2	30 ± 3	78 ± 3	126 ± 10
12G	2	47 ± 17	89 ± 28	131 ± 40
24G	3	68 ± 3	140 ± 12	213 ± 25

Table 3.1: Moduli of elasticity of cross-linking groups (mean plus s.e.m.) at different strains.

3.2.2 Type II Collagen Sponges

The type II collagen sponges were tested in the same manner as the type I sponges. The dimensions of the type II collagen test specimens were restricted, however, by the size of the sponges received from Geistlich Biomaterials. All of the type II specimens failed at very low stresses, and all failed at one of the clamped ends of the specimens. The resulting stress-strain relation appeared to be the result of the limitations of the equipment and the specimens rather than a true representation of the stress-strain behavior of the type II collagen sponges. Therefore, these data are not included in the results.

3.3 Fibroblasts

The patellar tendon digestion used to dissociate the tenocytes from their tissue resulted in a harvest of approximately 1.3 million cells per gram of patellar tendon tissue. The mass of the tissue was measured before the non-midsubstance tissue was dissected away.

Cells were passaged when confluence was reached. A typical culture flask yielded between 5 and 7 million cells at passage. Cells proliferated more rapidly with each passage.

3.4 Cell Seeding

3.4.1 Efficiency of Cell Seeding

Suspension of the cells in a small amount of culture medium (2.5×10^5 cells per 50 μl) allowed the full amount to the suspension to be pipetted onto the surface of the sponge. The "drying" step of removing excess medium from the sponges also allowed the cell suspension to more easily infiltrate the sponges. In some instances, however, a portion of the cell suspension spilled off of the sponges and onto the agarose coated wells. The swollen type II sponges appeared to absorb the suspension better than the

type I sponges.

Following the first post–seeding medium change, the cells remaining in the medium (and therefore not attached to the sponges) were counted. From these counts, it was determined that approximately 97% of cells were incorporated into the matrix or else attached to the upper walls of the culture wells, which were not coated with agarose. Cells did not attach to the agarose coating.

3.4.2 Infiltration of Cells into the Sponges

Infiltration behavior of cells into sponges was similar for sponges of all treatment groups. At 3 days post-seeding, H&E stained sections of seeded sponges showed that cells were primarily attached to the periphery of the sponges and the edge regions (Figure 2-4) of the sponges. Few cells were visible in the center portions of all sponge groups. By the 7th day in culture, H&E stained cross-sections revealed that the fibroblasts had migrated midway through the depth of the sponges (approximately 1.0 mm – 1.5 mm). Because cells had been seeded onto both flat surfaces of the sponges, it was assumed that the cells were migrating from both sides of the disk. Therefore, the greatest extent of migration was assumed to be one-half of the disk thickness, although it is possible that cells migrated from one surface to the opposite surface. At seven days after seeding, there were more cells at the edges of the disk, but the center was still sparsely populated.

Dense layers of cells were attached along the edges of the type I CG sponges by 14 days post-seeding. The DHT and ETH sponges in particular were surrounded with what appeared to be a multi-layered cell capsule, while the cell layers at the edges of the type II, UV and glutaraldehyde-treated sponges were not as thick and did not completely surround the sponges. Fibroblasts were attached to all sponges in the center of the disks (Figure 3-10), but in the DHT, and UV groups, the majority of cells in the disk were seen in the edge regions. Cells were more evenly distributed throughout the type II and glutaraldehyde-treated sponge groups. By the 21st day in culture, both the edge and center regions of sponges from all treatment groups had become densely populated with fibroblasts.

The DNA content of the sponges, reflecting the cell number, at each time period for each treatment group was quantified by DNA assay. The results of the assay are shown in Figure 3-9, and the DNA content is expressed as ng DNA per 100 μl of the papain digest. In the type II, UV, and glutaraldehyde cross-linked groups, the amount of DNA, and thus, the number of cells, increased from day 14 to day 21, while the DNA content decreased over the same time period for the ethanol and DHT group sponges. The differences in DNA content among all groups were statistically significant at 14 and 21 days with the exception of the UV group and 12G group at 14 days. DNA content was highest in type II sponges and lowest in DHT sponges. The DNA content in 12G and 24G sponges was similar, however, the DNA content in the 0.5G sponges was significantly greater than all CG sponge groups.

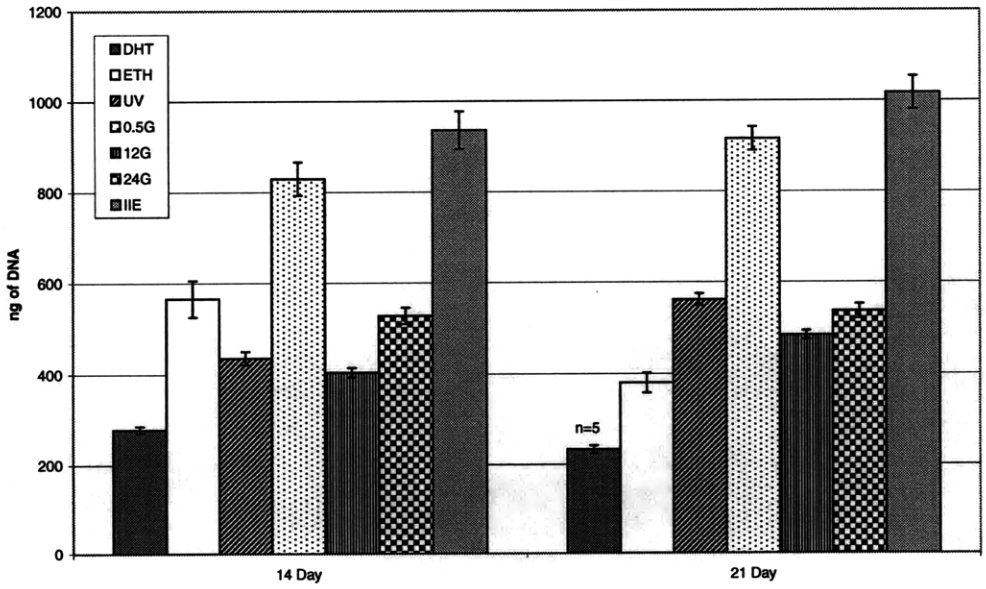

Figure 3-9: DNA content of collagen sponges at 14 and 21 days. DNA content is expressed as ng of DNA per 100 μl papain digest. Unless otherwise noted, n=6.

3.4.3 Cell Morphology

By the end of the first week in culture, cells at the periphery of all sponges were elongated along the edges of the sponges. For DHT, ethanol treated, UV irradiated, and 30-minute glutaraldehyde cross-linked groups, cells densely populated the edge region of the disks at 14 and 21 days post-seeding. These cells were primarily fusiform or ovoid, with the fusiform morphology more prevalent in the edge region. The cells in the center region of these disks were also both fusiform and ovoid, with a slightly higher percentage of ovoid cells (Figure 3-10). Very few spheroid cells were seen in either region of these disks.

Fibroblasts in the 12-hour and 24-hour glutaraldehyde cross-linked sponges were primarily fusiform in both the edge and center regions after 14 days in culture (Figure 3-11). Prior to 14 days, the center regions of the sponges were sparsely populated with primarily ovoid cells, and the edges were populated by a few layers of elongated cells.

Cell morphology in type II collagen sponges was similar to the morphology in the DHT and ethanol groups, with a slightly higher percentage of cells at early time periods which were spheroid in shape.

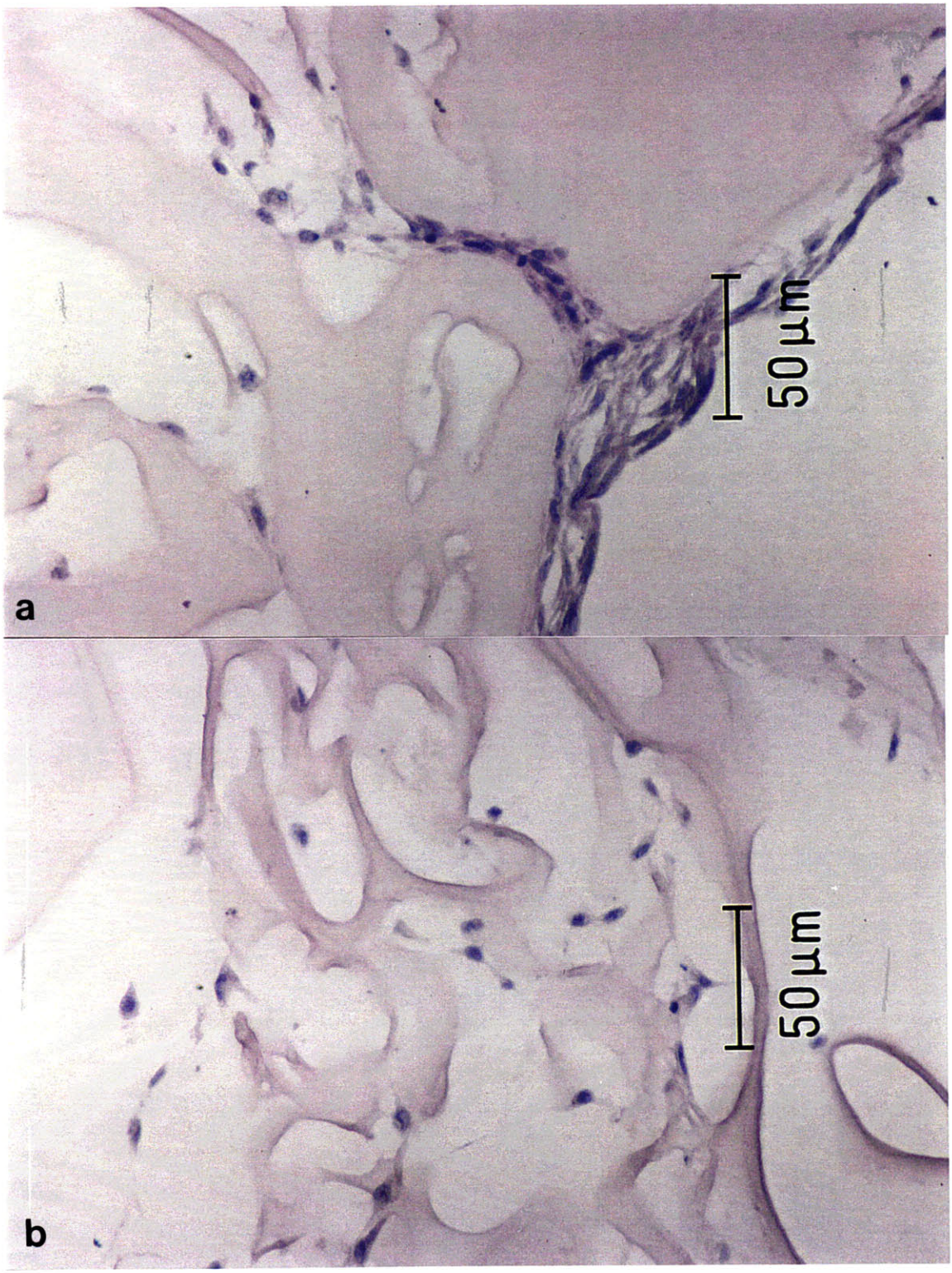

Figure 3-10: Light micrograph of typical cell distribution and morphology in CG sponges at (A) the edge and (B) center of the sponge. H&E stained section of an ethanol-treated fibroblast-seeded CG sponge at 14 days post-seeding.

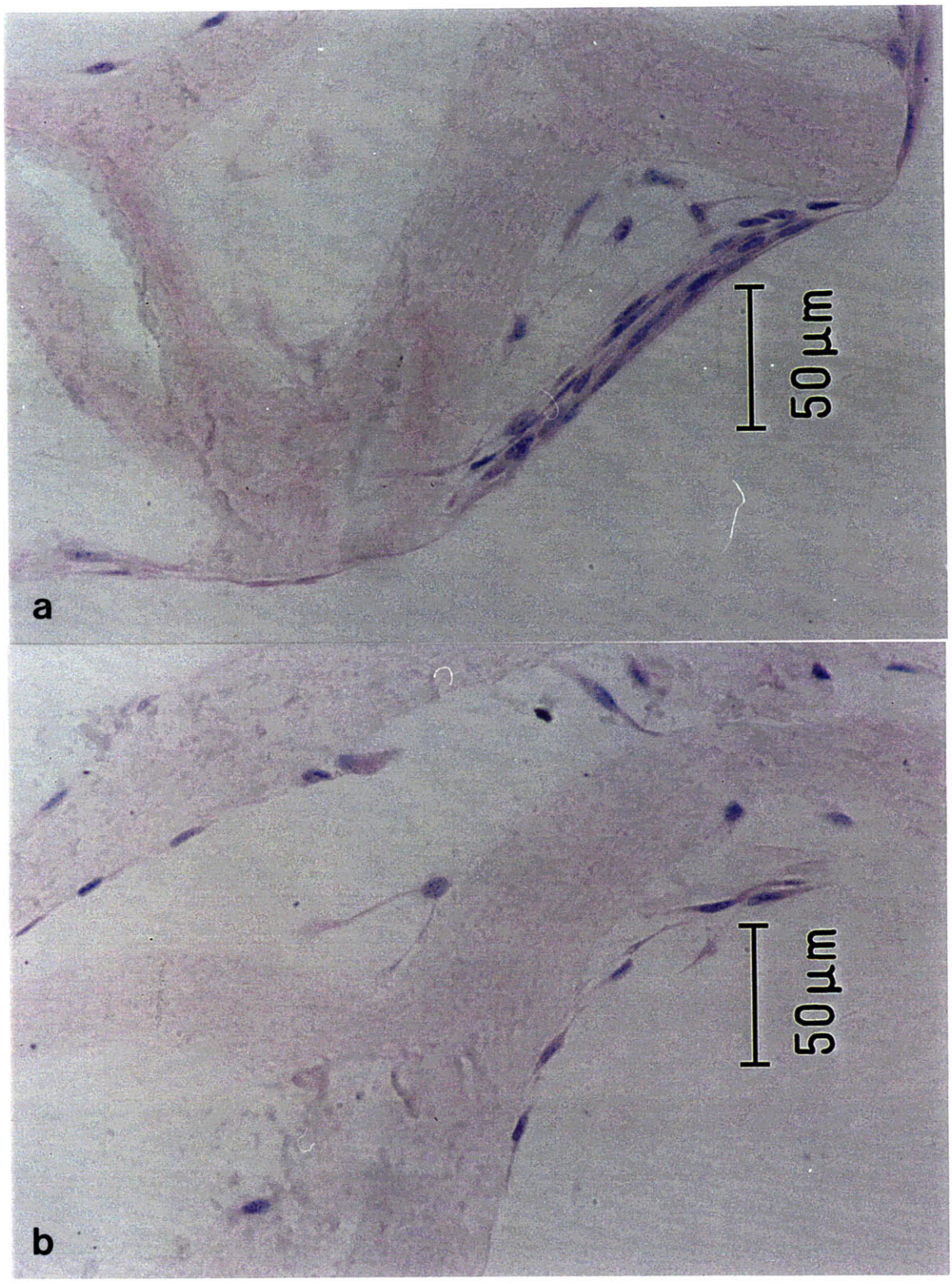

Figure 3-11: Light micrograph of cell distribution and morphology in a CG sponge at (A) the edge and (B) center of the sponge. H&E stained section of a 24-hour glutaraldehyde cross-linked fibroblast-seeded CG sponge at 21 days post-seeding.

3.5 Cell-Mediated Contraction of Sponges

3.5.1 Observations

Cell-seeded sponges from the dehydrothermal (DHT) group and ethanol-treated (ETH) group had undergone visible contraction by the third day in culture. Ultraviolet irradiated (UV) sponges had contracted visibly by 7 days in culture, and contraction was evident in 30-minute glutaraldehyde (0.5G) cross-linked sponges by the 14th day in culture. Sponges which had been cross-linked for 12 and 24 hours in glutaraldehyde (12G and 24G, respectively) had not visibly contracted after 21 days. A previous study [37] of cell-seeded type I CG sponges had noted a curling up of the edges of the sponge. Sponges from all groups in this experiment, however, appeared to contract uniformly and no curling up of the edges was noted.

Type II collagen sponges appeared smaller after three days in culture. However, after calculating the disk diameter, it was clear that the apparent decrease in size was actually the abatement of the swelling of the disks. The original measurement of the disk was made while the disk was still swollen, so it appears that the disks contracted to 70-75% of their original diameter after three days. The actual mean disk diameter after three days was 9.2 $\pm$ 0.4 mm for seeded type II sponges, and 9.2 $\pm$ 0.5 mm for unseeded control sponges, which was near the original size of the disks (9 mm) cut from the Chondrocell sponges. Type II sponges also became very fragile in culture and were difficult to handle. The smaller number of samples (n) at some time points is a result of type II sponges falling apart before they could be measured.

3.5.2 Imaging of Sponge Contraction

Contraction of sponge disks was measured as described in section 2.5. Examples of a sponge image as recorded prior to seeding, the processed image file showing the disk areas calculated prior to seeding, the same sponge as recorded at sacrifice, and the processed image for that sponge are shown in Figure 3-12. The white area of the processed file was considered the disk area, and the number of white pixels

was counted. The white pixel area (A) was then compared to a similar pixel area calculated for a dime (U. S. currency, $0.10, 17.84 mm diameter) in order to estimate the size of the disk diameter (d) using the equation:

$$d = \sqrt{\frac{4A}{\pi}}$$

An example of a disk which underwent minimal contraction is shown in Figure 3-13.

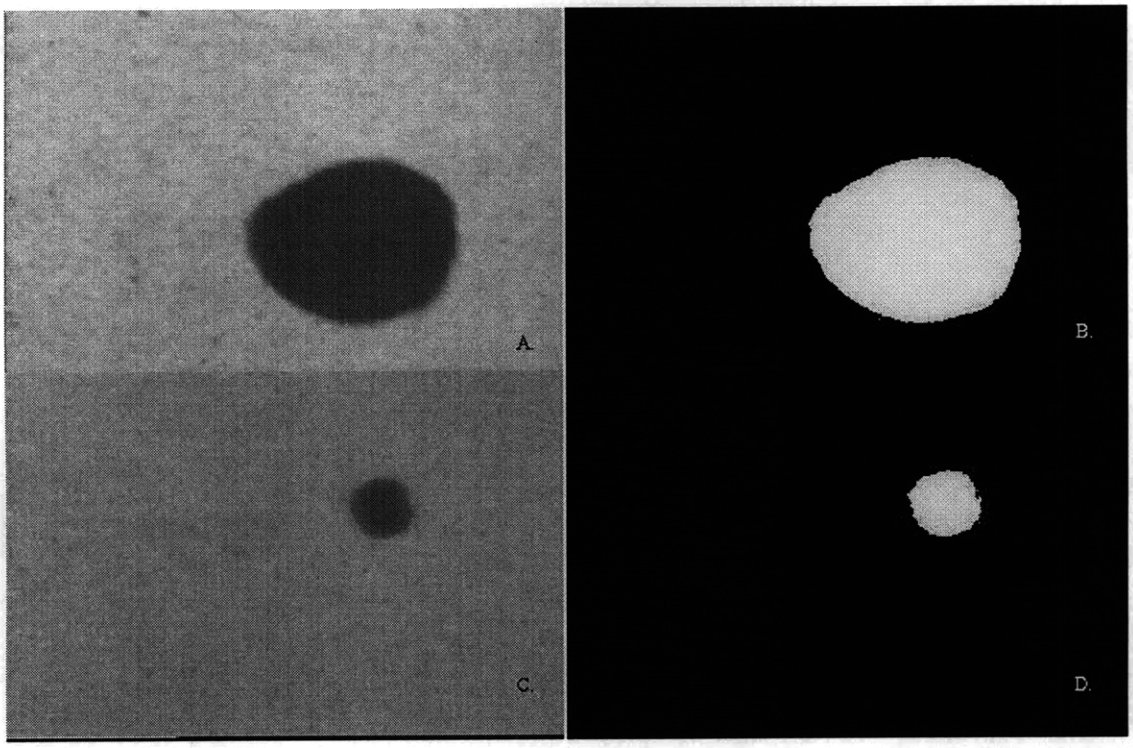

Figure 3-12: Sponge contraction images. A: JPEG image of dehydrothermal (DHT) treated sponge prior to seeding. B: Processed image of DHT treated sponge prior to seeding. The black area is considered background, and the white area is counted as the disk area. C: JPEG image of DHT treated sponge at 21 days post-seeding. D: Processed image of DHT treated sponge at 21 days post-seeding. Sponge has been contracted to 38% of its original diameter.

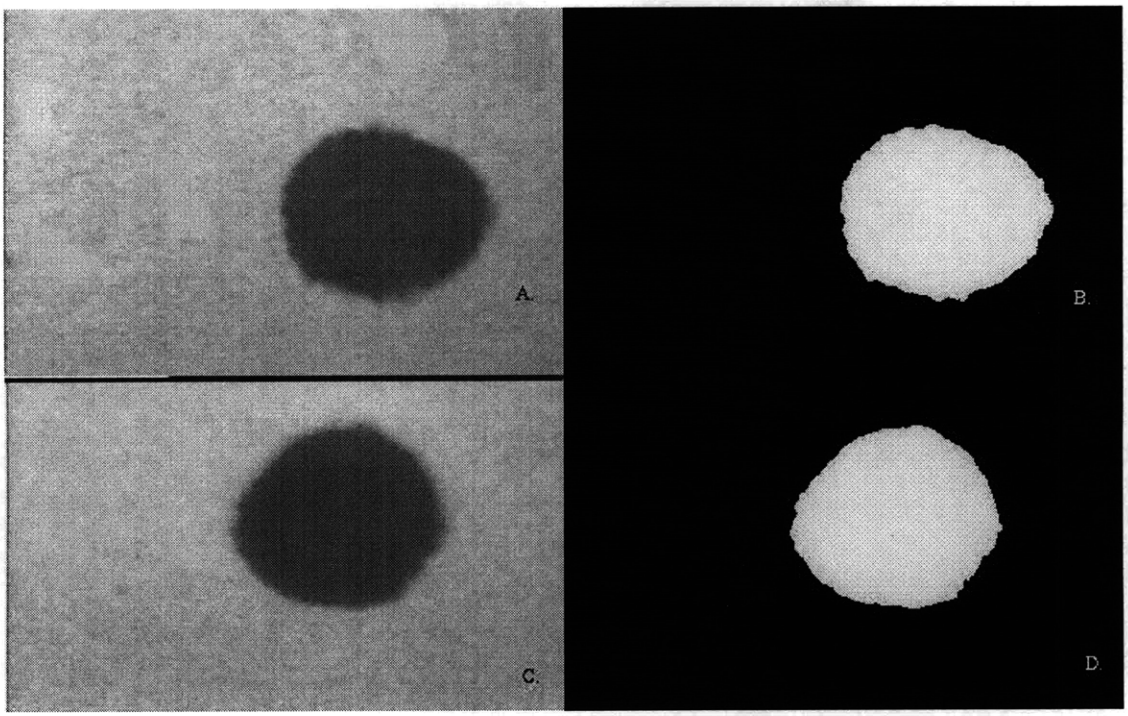

Figure 3-13: Sponge contraction images. A: JPEG image of 24 hour glutaraldehyde (24G) treated sponge prior to seeding. B: Processed image of 24G treated sponge prior to seeding. The black area is considered background, and the white area is counted as the disk area. C: JPEG image of 24G treated sponge at 14 days post-seeding. D: Processed image of 24G treated sponge at 14 days post-seeding. Sponge has been contracted to 97% of its original diameter.

3.5.3 Measurement of Contraction of Sponges

The change in seeded and control sponge diameters of each treatment group over time is shown in Figures 3-14 – 3-20. Unless otherwise noted, n=6. The contraction of seeded sponges from all groups are compared in Figure 3-21. The contraction curves of unseeded control sponges from all groups is compared in Figure 3-22.

Reduction in diameter of unseeded control sponges from the DHT and ETH group was evident at 3 days. This shrinkage of the control sponges in these groups was almost equal to the contraction of the seeded sponges for seven days. After that time, the shrinkage in the control groups leveled off while the seeded sponges continued to contract. Unseeded controls in the UV group contracted slightly by 14 days, while

the glutaraldehyde-treated controls did not contract significantly throughout the 21 day course of the experiment.

Tenocyte-seeded DHT sponges contracted to 37 ± 1% of their original diameter, and ethanol treated sponges contracted to 40 ± 2% of their original diameter after 21 days. UV cross-linked sponges were contracted to 80 ± 3% at 21 days.

Contraction in glutaraldehyde-treated sponges varied with the length of cross-linking time. Following 21 days in culture, seeded sponges cross-linked for 30 minutes were contracted to 72 ± 3% of their original diameter, while the average diameters of the 12-hour and 24-hour cross-linked sponges fell to 97 ± 1% and 98 ± 1% of their original values, respectively.

As described above, the apparent contraction of type II collagen sponges at three days was explained by the subsidence of swelling in the sponges. After three days, seeded and control sponge diameters remained at approximately 91% to 98% of the original diameter before rehydration.

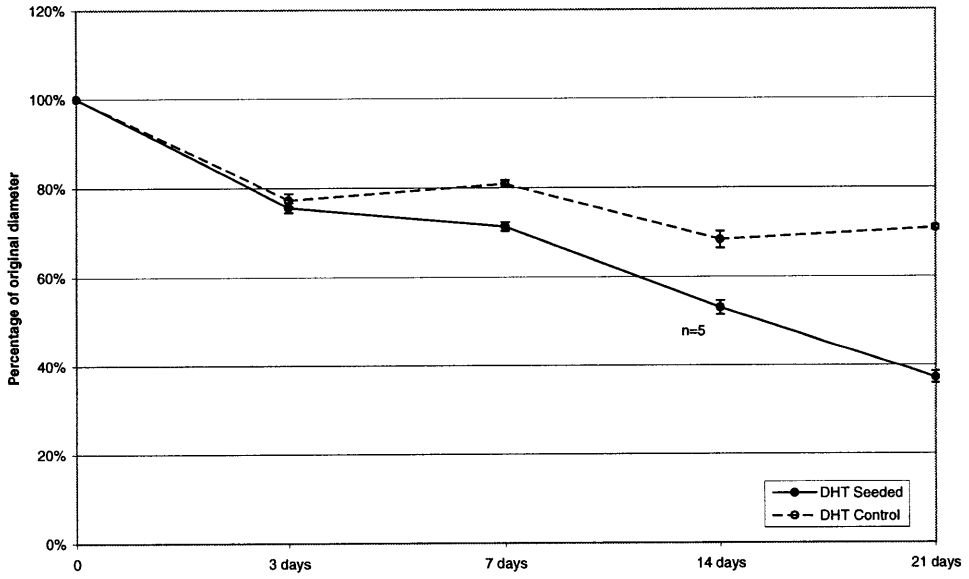

Figure 3-14: Shrinkage of dehydrothermal (DHT) cross-linked sponges at 3, 7, 14, and 21 days post-seeding (mean ± s.e.m.). Differences in contraction between seeded and control sponges at 7, 14, and 21 days were significant ($p \ll 0.001$).

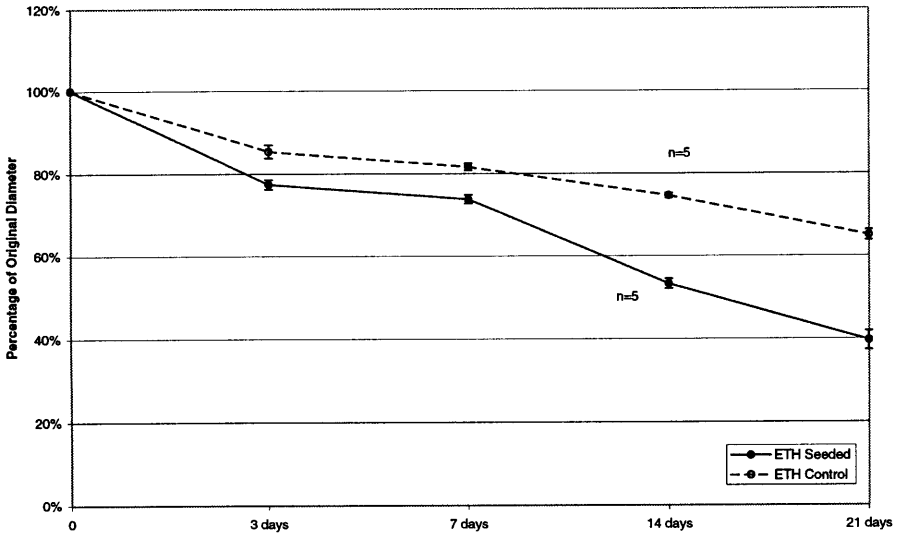

Figure 3-15: Shrinkage of ethanol treated (ETH) sponges at 3, 7, 14, and 21 days post-seeding (mean $\pm$ s.e.m.). Differences in contraction between seeded and control sponges were significant for all time periods ($p \ll 0.05$).

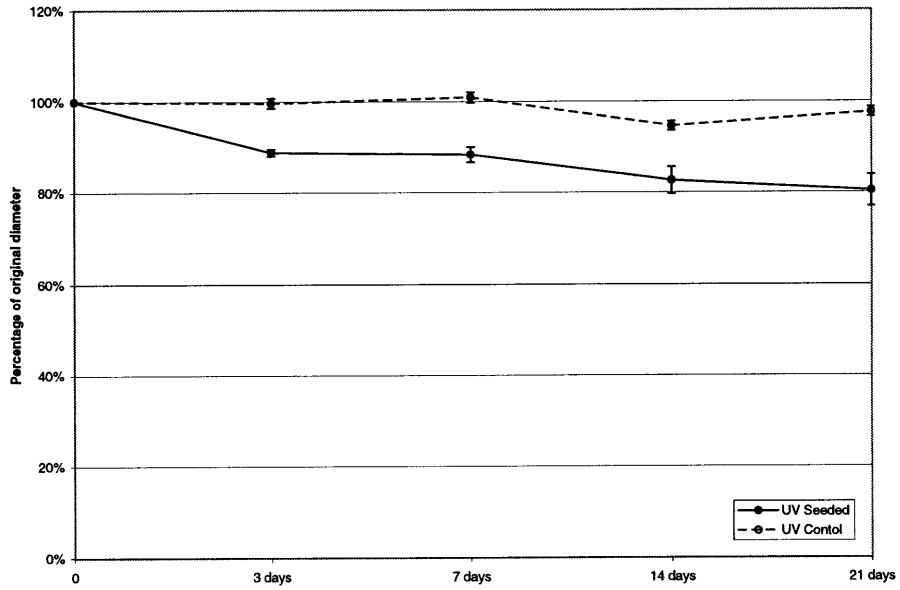

Figure 3-16: Shrinkage of ultraviolet light (UV) cross-linked sponges at 3, 7, 14, and 21 days post-seeding (mean $\pm$ s.e.m.). Differences in contraction between seeded and control sponges were significant for all time periods ($p \ll 0.05$).

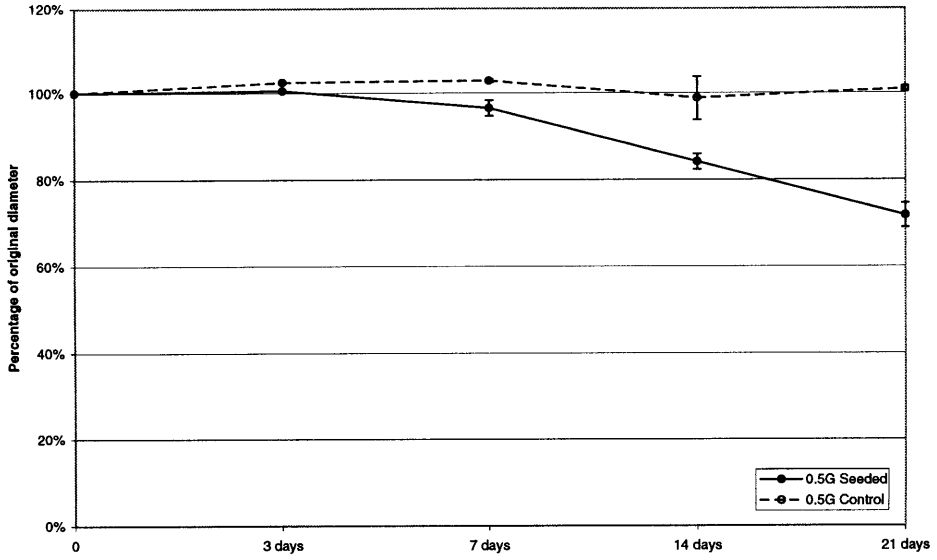

Figure 3-17: Shrinkage of 30-minute glutaraldehyde (0.5G) cross-linked sponges at 3, 7, 14, and 21 days post-seeding (mean $\pm$ s.e.m.). Differences in contraction between seeded and control sponges were significant for all time periods ($p < 0.05$).

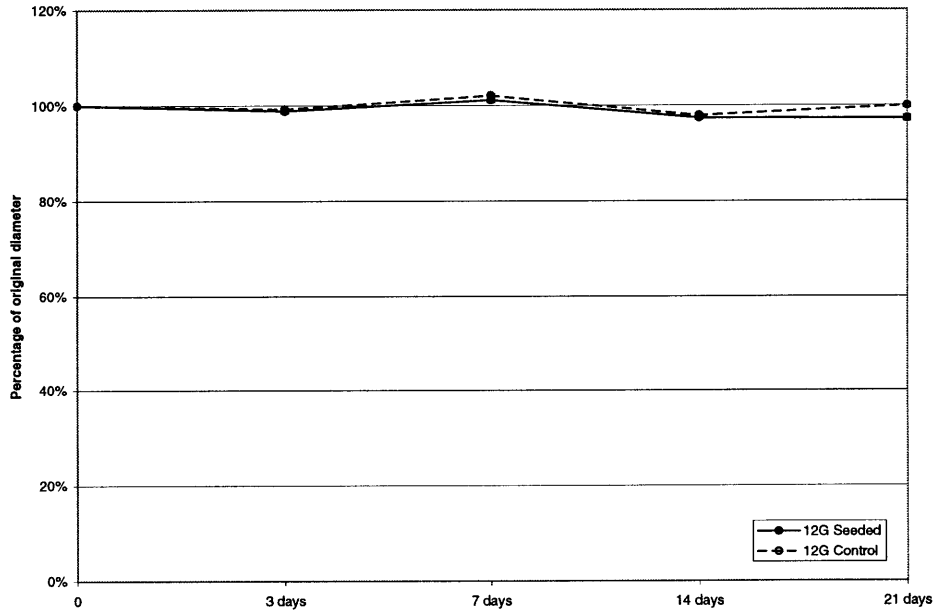

Figure 3-18: Shrinkage of 12-hour glutaraldehyde (12G) cross-linked sponges at 3, 7, 14, and 21 days post-seeding (mean $\pm$ s.e.m.). Differences between seeded and control sponges were significant at 21 days ($p \ll 0.05$).

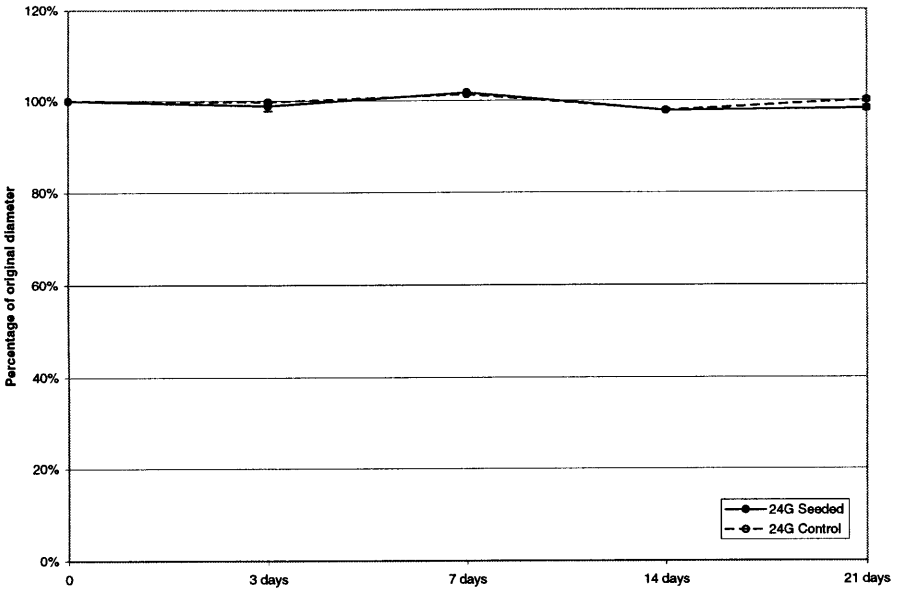

Figure 3-19: Shrinkage of 24-hour glutaraldehyde (24G) cross-linked sponges at 3, 7, 14, and 21 days post-seeding (mean $\pm$ s.e.m.) Differences between seeded and control sponges were significant at 21 days ($p < 0.05$).

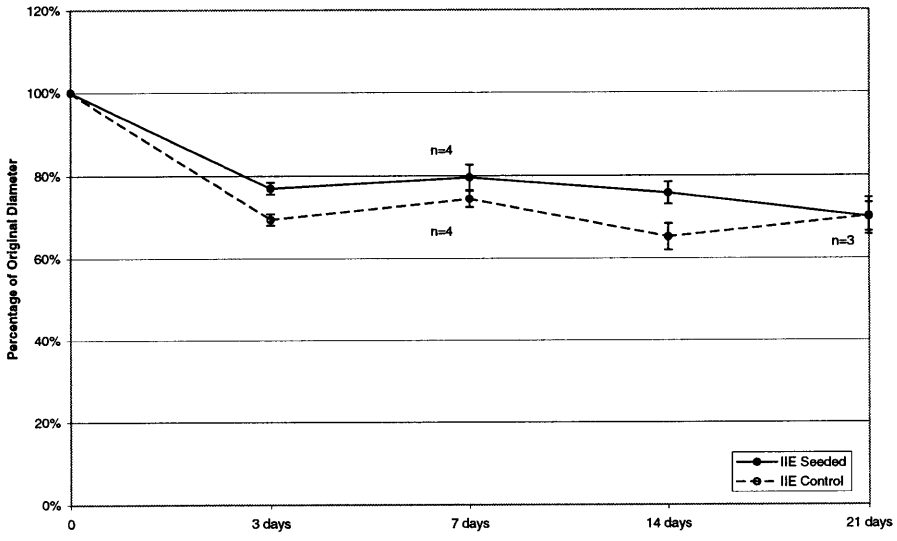

Figure 3-20: Shrinkage of type II collagen (IIE) sponges at 3, 7, 14, and 21 days post-seeding (mean $\pm$ s.e.m.). Differences in contraction between seeded and control sponges were only significant ($p < 0.05$) at 3 and 14 days. Note that shrinkage in the control sponges is greater than in the seeded sponges at these time periods.

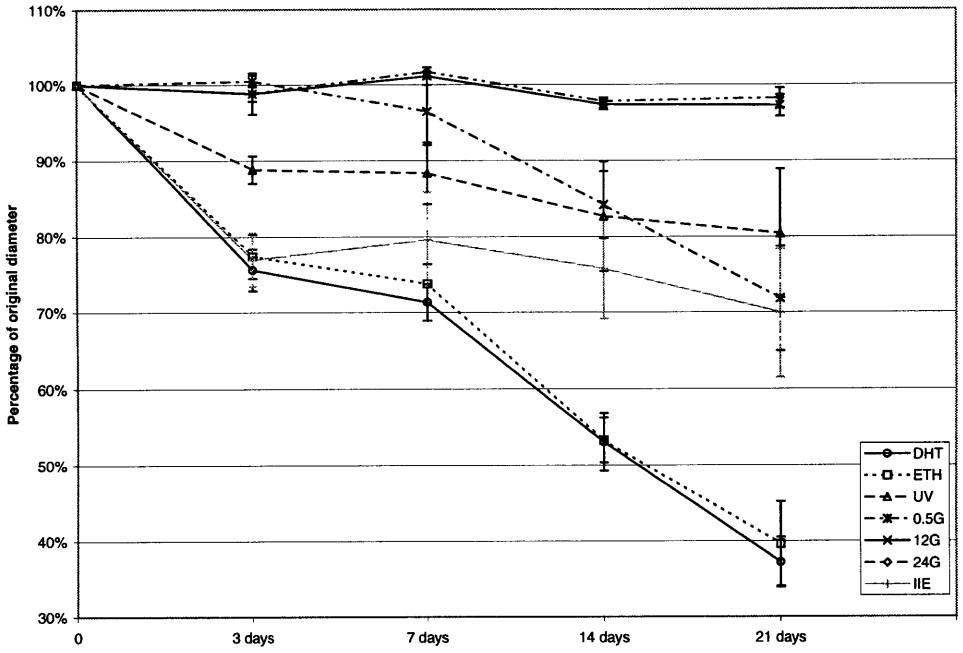

Figure 3-21: Shrinkage of fibroblast-seeded sponges at 3, 7, 14, and 21 days post-seeding.

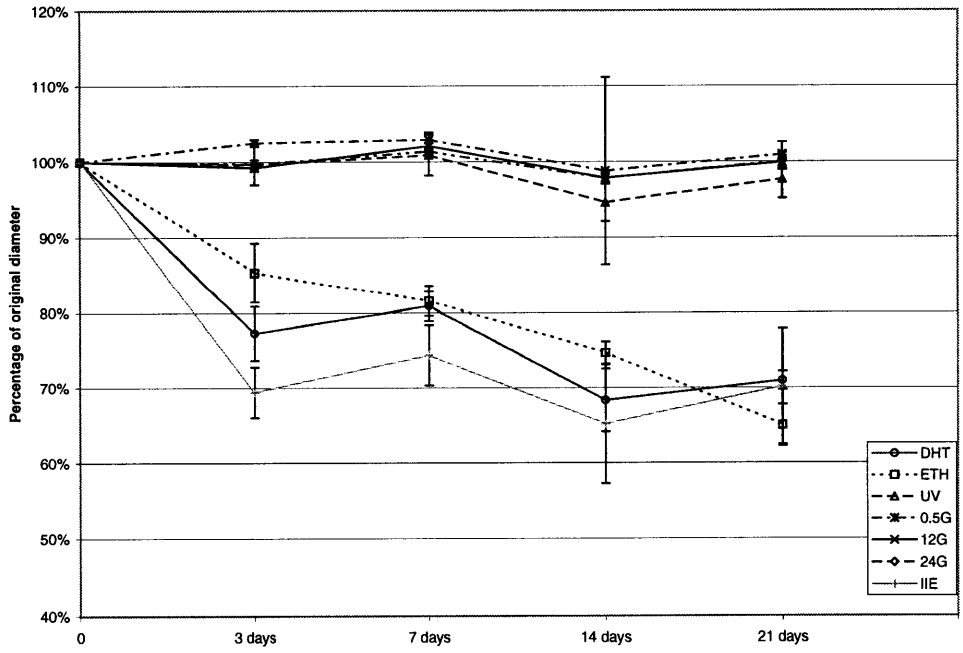

Figure 3-22: Shrinkage of unseeded (control) sponges at 3, 7, 14, and 21 days post-seeding.

3.5.4 Changes in Pore Size

Light microscopy was used to investigate the change in size of the pores of both the seeded and unseeded collagen sponges. The range of pore diameters and average pore diameter of DHT and ETH sponges appeared qualitatively to have decreased slightly. Pores of type II collagen, UV and glutaraldehyde cross-linked sponges underwent no apparent shrinkage.

A photomicrograph of an ethanol treated sponge prior to seeding shows the open pore structure of the sponge throughout the disk (Figure 3-23 A). After three days in culture, few changes in the sponge pores are visible (Figure 3-23 B). By the seventh day in culture, the pores have become visibly contracted at the edges of the disk (Figure 3-24 A), and at 14 days, clear differences can be seen between the pore size at the edge and center of the sponge (Figure 3-24 B). Pores at the edge and center of the sponge at 21 days have been highly contracted (Figure 3-25 A).

In all sponges in which significant contraction occurred, the pores at the edges of the sponge became contracted before pores in the center of the sponges. When only slight contraction was noted, a visible change in the pores was not seen at either the edges or the center of the disk (Figure 3-25 B).

3.5.5 Cell-Mediated Contraction

Cell-mediated contraction was computed as the difference in contraction between the seeded and control sponges for each time period (Figure 3-26). The cell-mediated contraction was then divided by the mean DNA content of the sponges. Figure 3-27 compares the cell-mediated contraction which has been normalized by DNA content for each treatment group at 14 and 21 days. Although overall contraction of seeded DHT group sponges and seeded ETH group sponges are similar at 21 days (approximately 37% and 40% of original diameter, respectively), when the cell-mediated contraction at 21 days for these groups is calculated, a large difference is noted. Also worth noting is that the contraction in the glutaraldehyde-treated groups (albeit small) is entirely cell-mediated. The unseeded sponges undergo no significant shrinkage, so the contraction seen in the fibroblast populated sponges is caused entirely

by the cells. The cell-mediated contraction in the type II sponges is represented as "negative" contraction because the shrinkage in the control specimens at some time periods was greater than that of the seeded specimens.

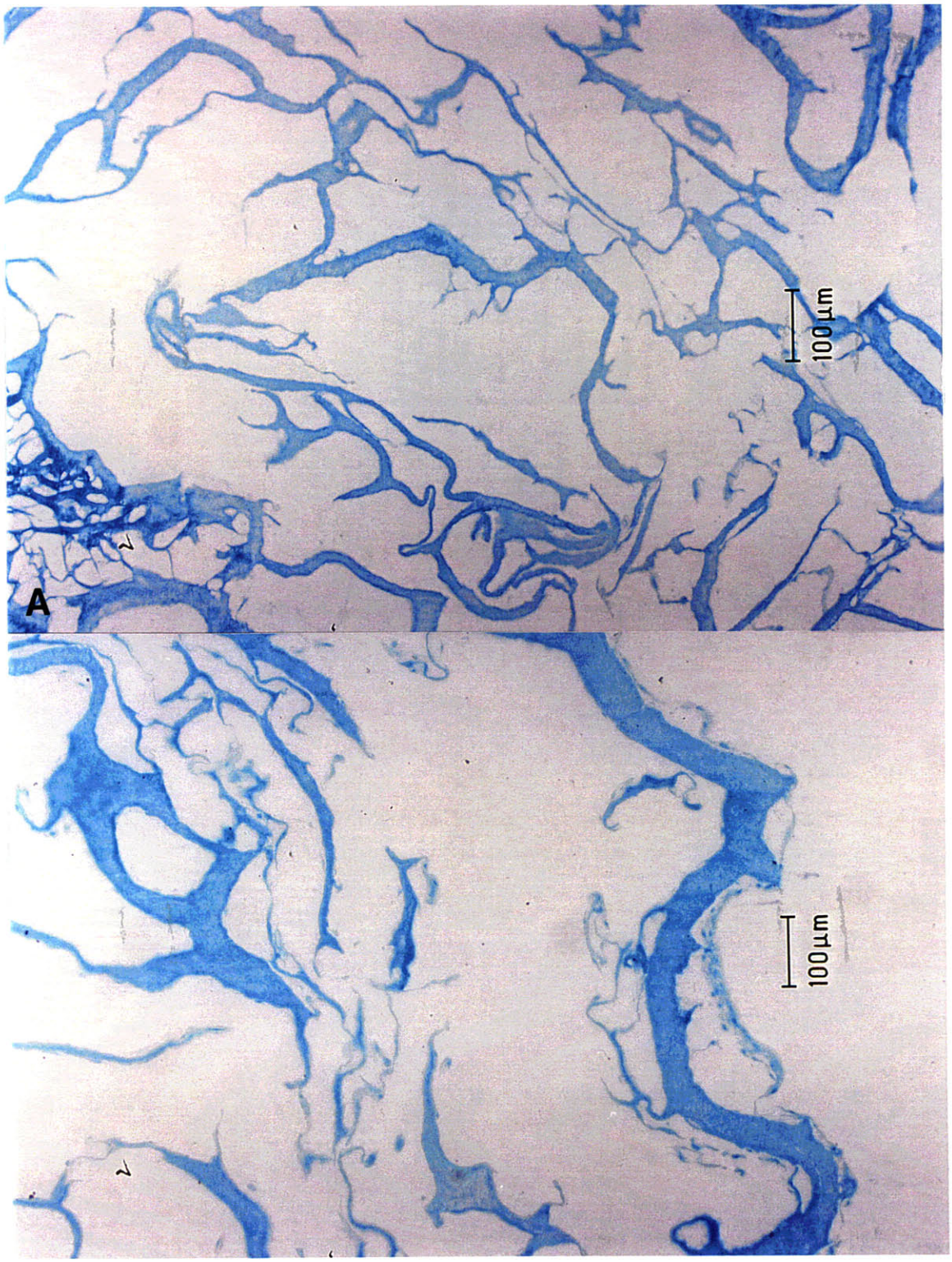

Figure 3-23: Light micrograph of analine blue stained section of ETH sponge showing sponge pores (A) prior to seeding and (B) at 3 days post-seeding.

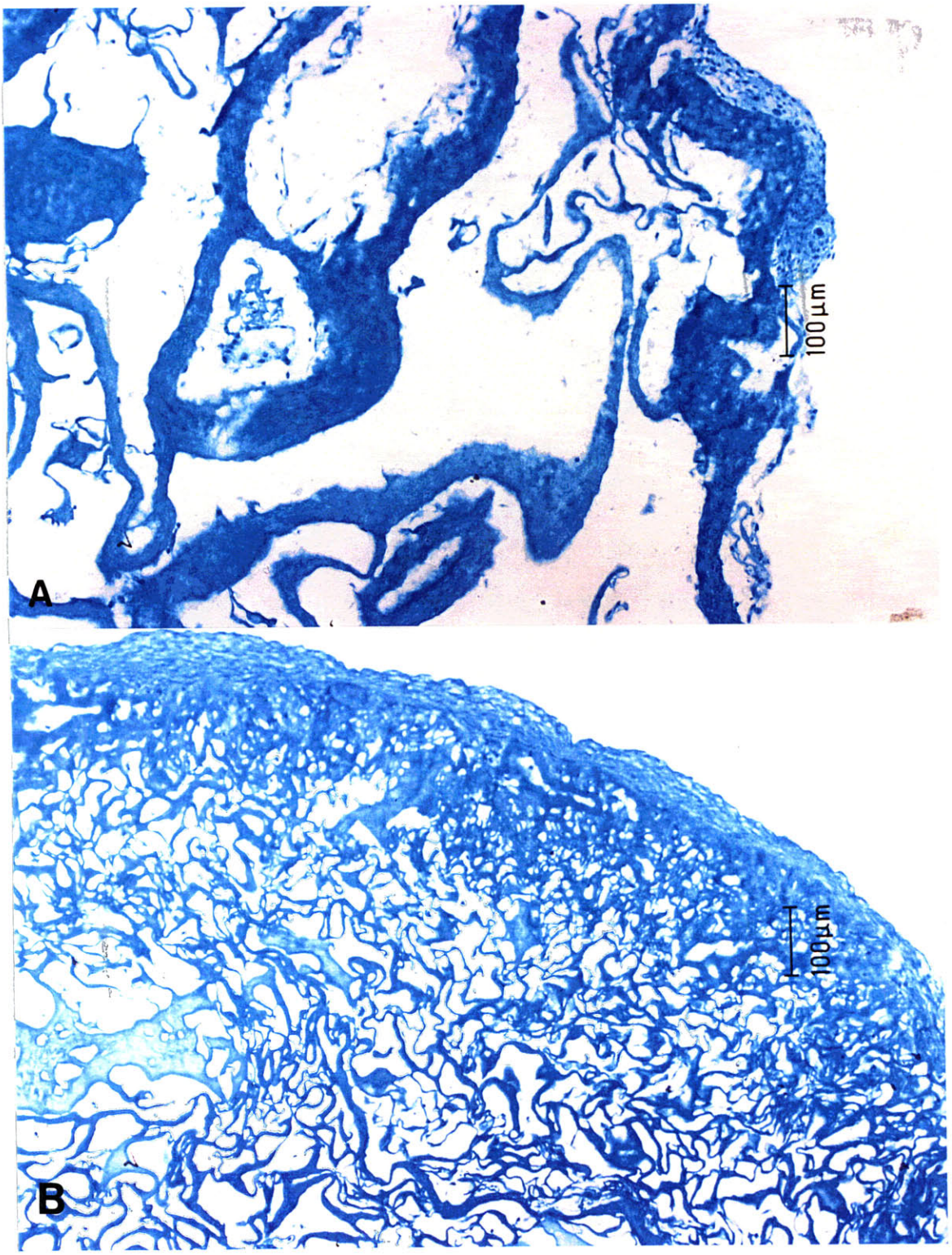

Figure 3-24: Light micrograph of analine blue stained section of ETH sponge showing sponge pores (A) at 7 days post-seeding and (B) at 14 days post-seeding.

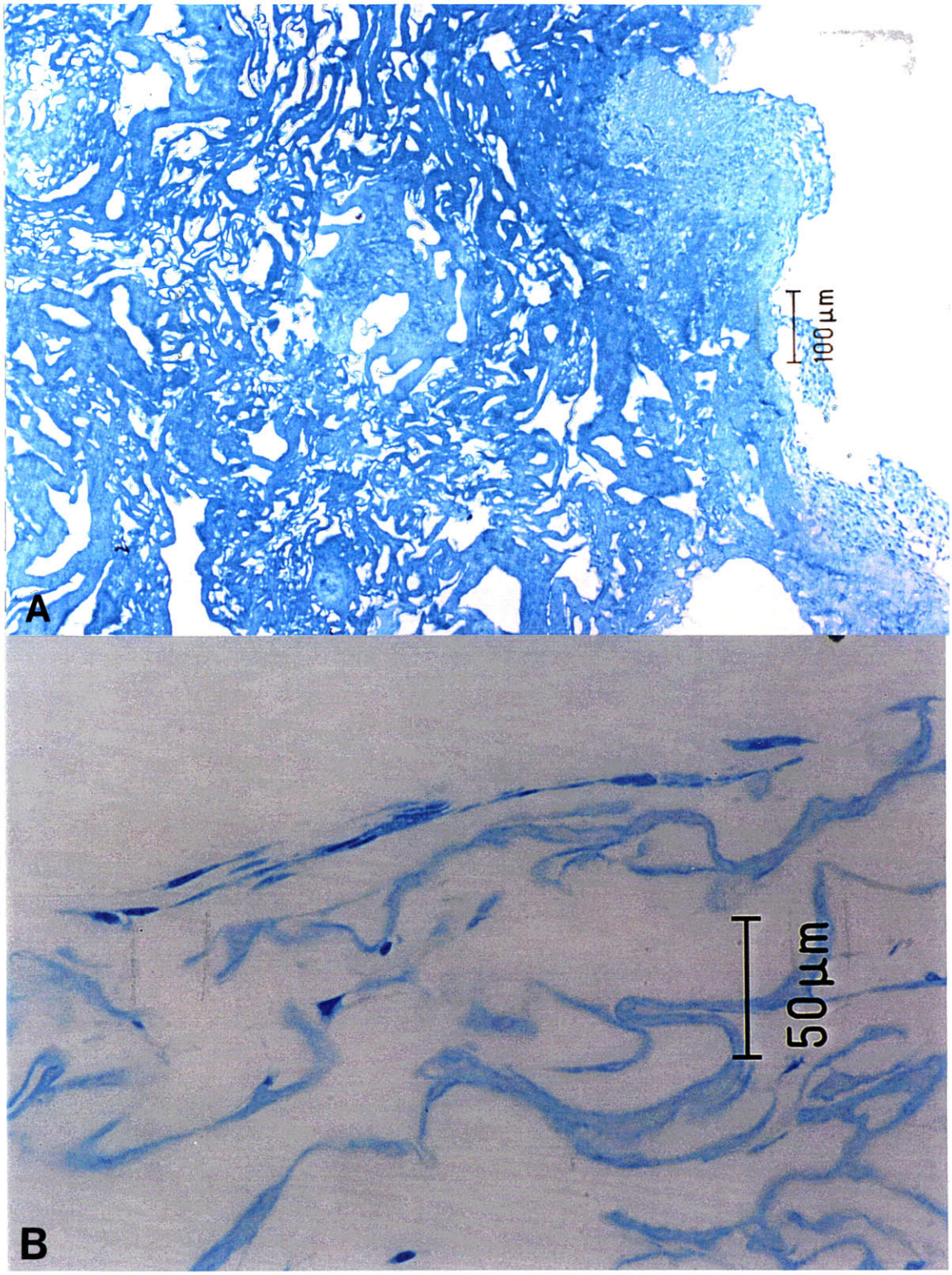

Figure 3-25: Light micrograph of analine blue stained section of (A) ETH sponge and (B) 24G sponge showing pore structure at 21 days post-seeding.

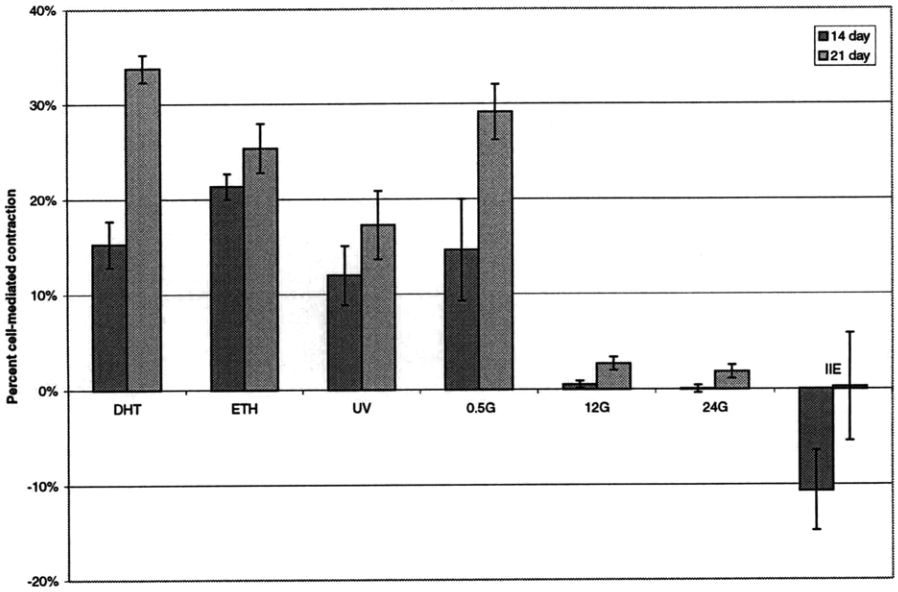

Figure 3-26: Cell-mediated contraction (percent difference in contraction of control and seeded sponges) at 14 and 21 days.

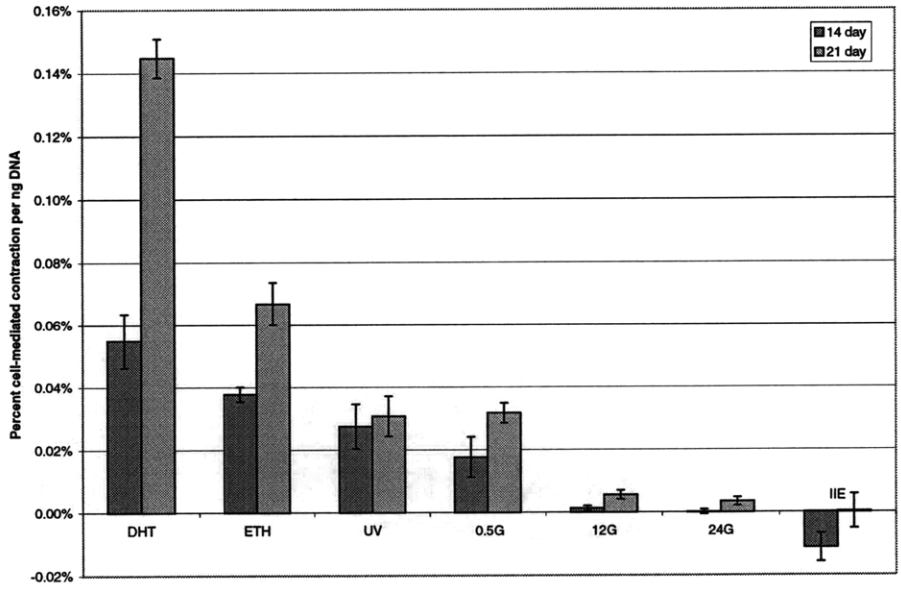

Figure 3-27: Cell-mediated contraction (percent difference in contraction of control and seeded sponges) per ng DNA in collagen sponges at 14 and 21 days. Contraction was divided by the mean DNA content without taking the deviation of the DNA content into account.

3.6 Effect of Apparent Modulus of Elasticity on Cell-Mediated Contraction

The mean cell-mediated contraction of the type I CG sponges from each treatment group at 21 days post-seeding was plotted versus the mean modulus of elasticity of the treatment groups at 10% strain (Figure 3-28) and 15% strain (Figure 3-29). A linear regression was performed to determine a relation between modulus of elasticity and cell-mediated contraction.

The linear regression for each resulted in a line with a negative slope, and the R^2 values for the regression at 10% and 15% strain were 0.64 and 0.72, respectively. The p-values for the regression were 0.032 for 15% strain and 0.055 for 10% strain.

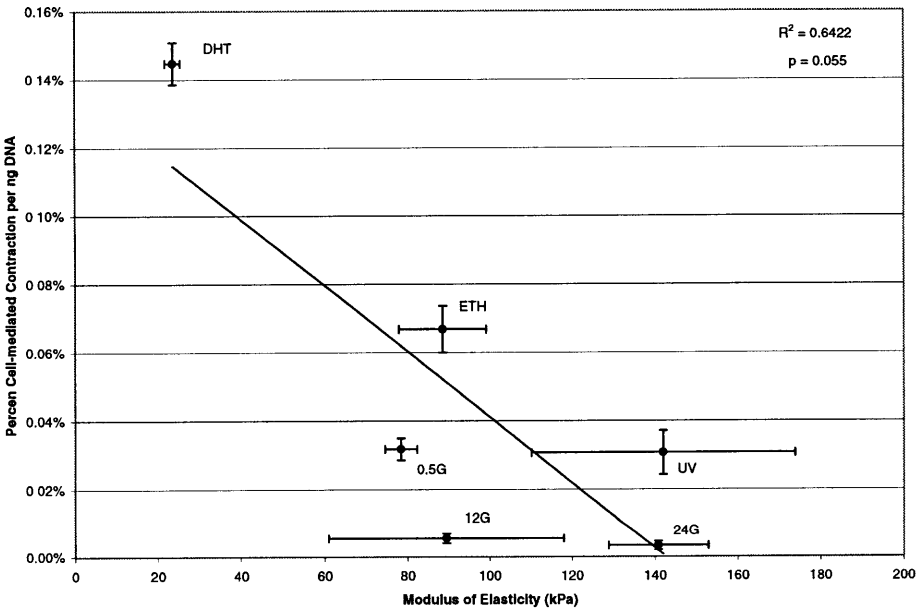

Figure 3-28: Cell-mediated contraction at 21 days as a function of modulus of elasticity at 10% strain.

3.7 Presence of Myofibroblasts

The presence of myofibroblasts was determined by immunohistochemical staining for alpha-smooth muscle actin. Figure 3-30 shows an example of positive staining for

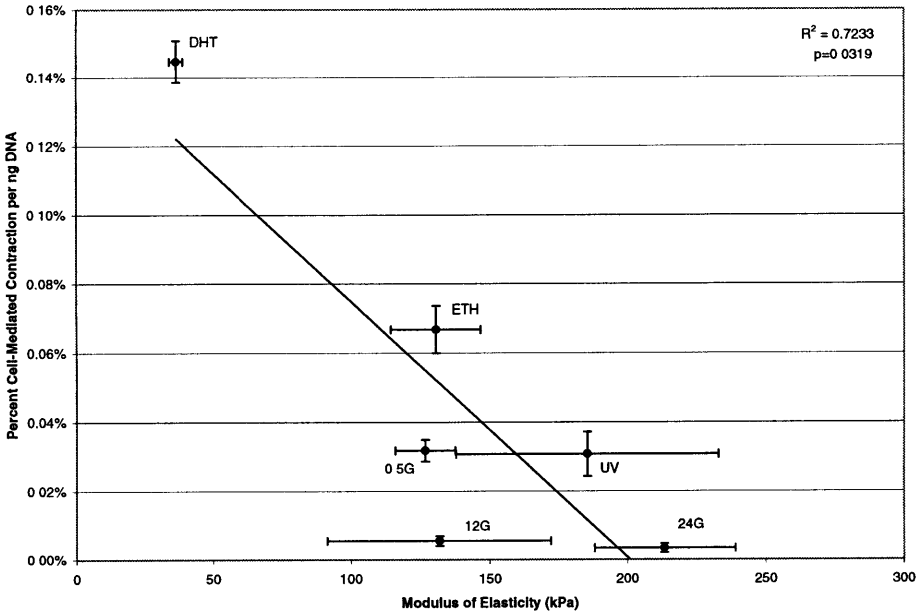

Figure 3-29: Cell-mediated contraction at 21 days as a function of modulus of elasticity at 15% strain.

this actin isoform (A) and a negative control (B). Myofibroblasts were found in all treatment groups at all time periods. The mean percentage of positively stained cells in the edge and center regions of some sponge groups was determined by counting cells from five random areas of four histological sections of two specimens from the same group. Mean percentages for the groups analyzed are shown in Table 3.2. In sponges which were contracted to a large degree, the percentage of positively stained cells appeared to peak at 14 days, and then drop slightly at 21 days.

Photomicrographs showing the positive staining in various sponge types are presented in Figures 3-31 – 3-32.

	3 days		7 days		14 days		21 days	
Group	Edge	Center	Edge	Center	Edge	Center	Edge	Center
DHT	90%	85%	93%	91%	97%	90%	91%	90%
ETH	92%	90%	97%	90%	99%	96%	94%	95%
24G	94%	95%	97%	94%	98%	99%	97%	99%

Table 3.2: Mean percentage of cells stained positive for α-smooth muscle actin.

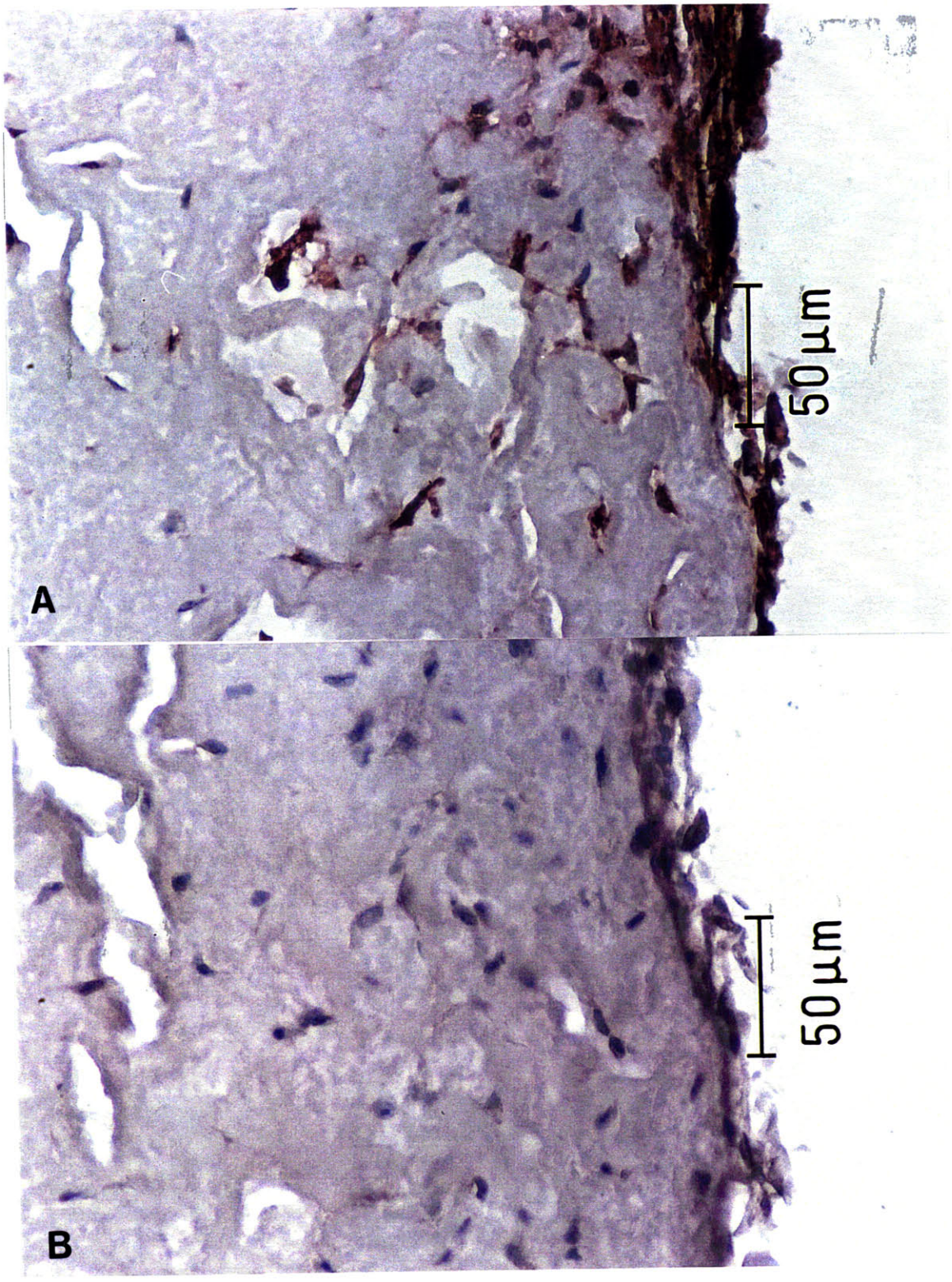

Figure 3-30: Light micrograph of immunohistochemical stain for α-smooth muscle actin (A) positive stain, and (B) negative control. Edge of DHT sponge at 21 days.

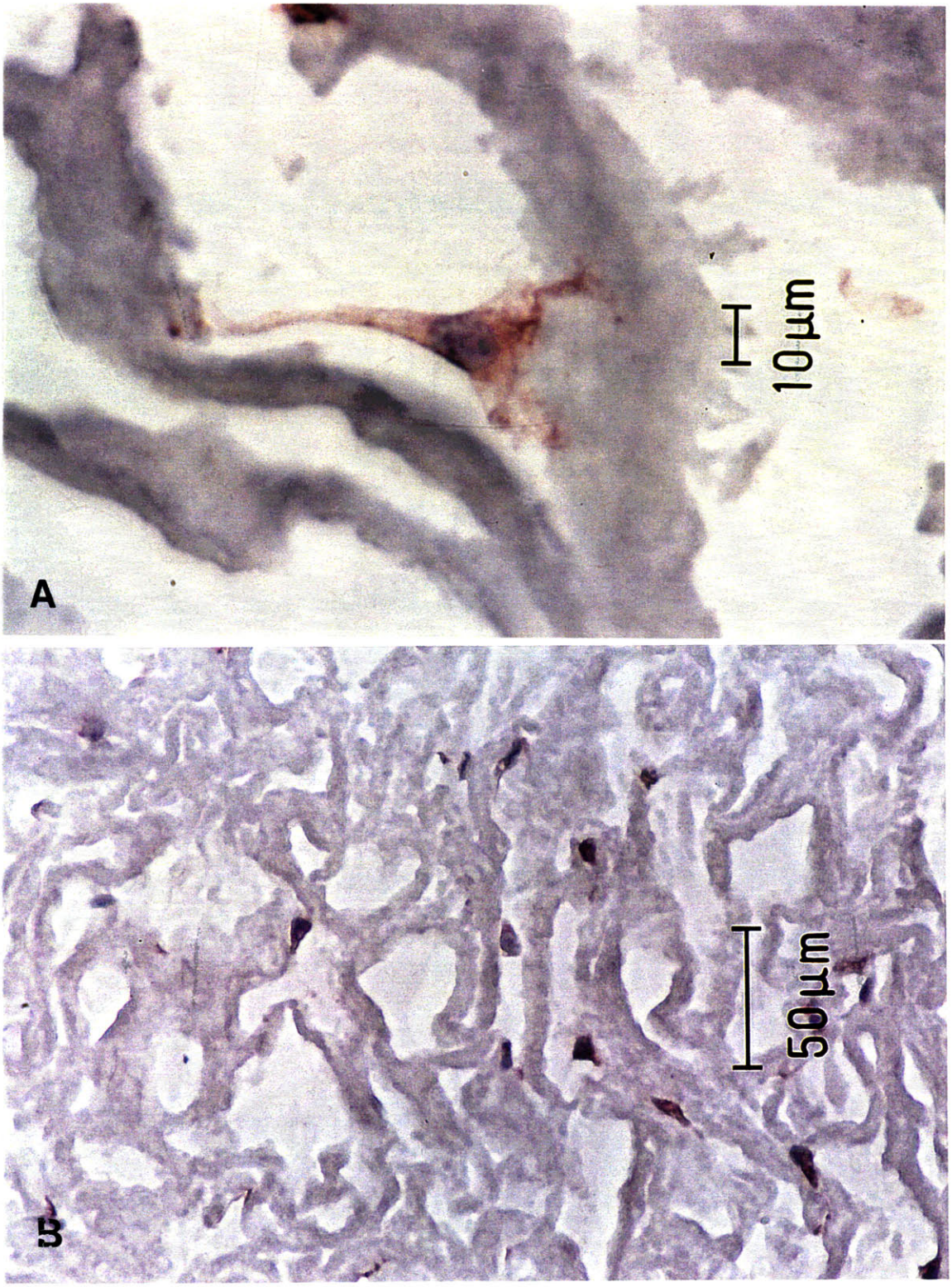

Figure 3-31: Light micrograph of immunohistochemical stain for α-smooth muscle actin in the center of a DHT sponge at 14 days (A) High-magnification and (B) lower magnification.

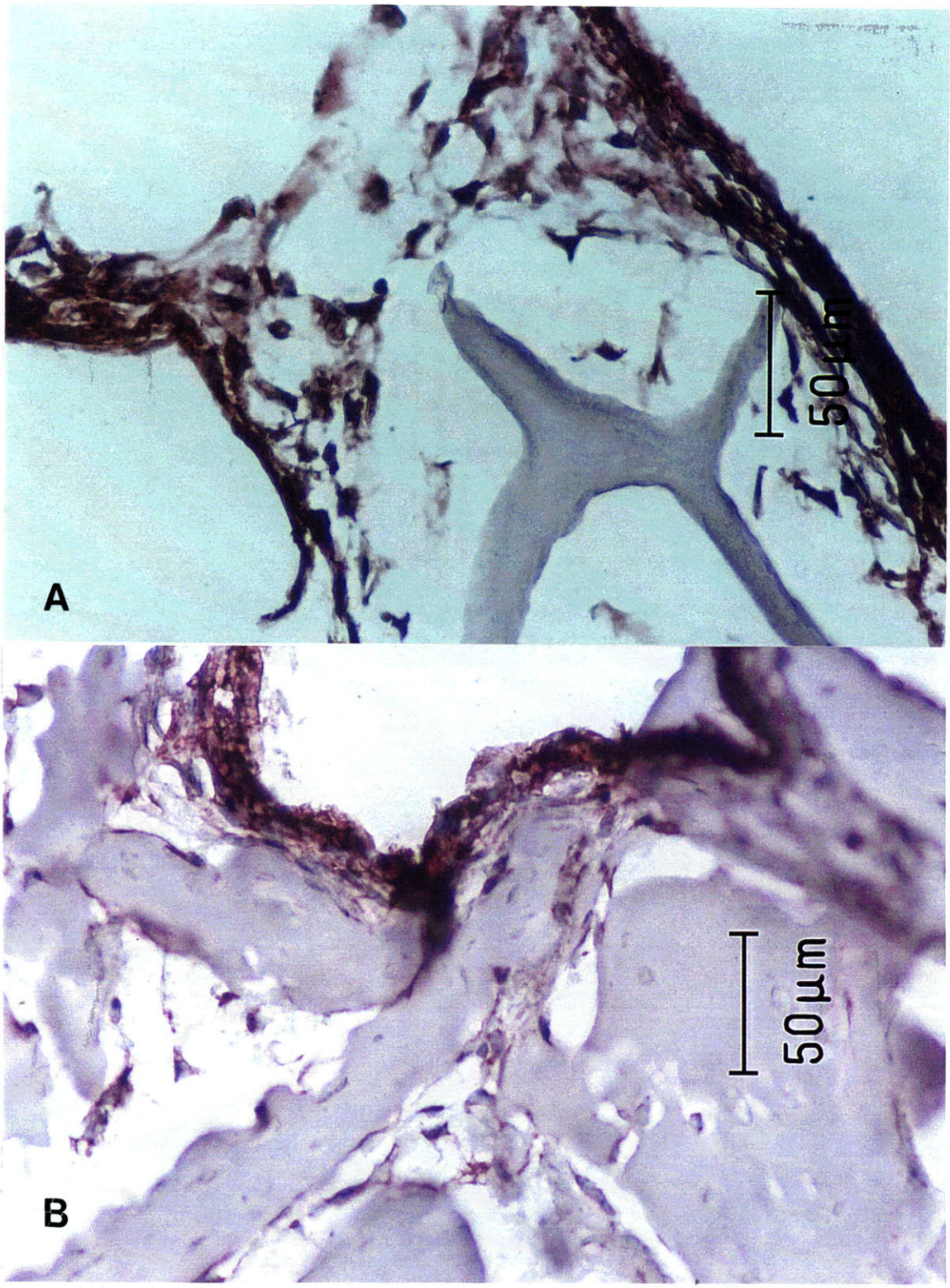

Figure 3-32: Light micrograph of immunohistochemical stain for α-smooth muscle actin in (A) 24-hour glutaraldehyde cross-linked sponge and (B) type II collagen sponge at 21 days.

Chapter 4

Discussion and Conclusions

The goal of this thesis was to determine the effect of the apparent modulus of elasticity of a CG sponge on the ability of seeded tendon cells to contract it. Contraction of sponges to be used as regeneration scaffolds is problematic in that the pores of sponges may be contracted such that cells can no longer migrate within them. In addition, contraction can affect the shape and size of the sponge, making it difficult or impossible to implant in a wound site, or causing it to separate from the host tissue before ingrowth can occur. By determining the effect of sponge stiffness on cell-mediated contraction of sponges, the minimum stiffness necessary to resist cell contraction for a particular cell type and density was determined. The use of different cross-linking methods also provided a comparison between physical and chemical cross-linking methods, and a basis for determining how physical cross-linking may be used instead of cross-linking with potentially cytotoxic chemicals.

One important finding of this thesis is that tendon cells *in vitro* are capable of contracting collagen sponges. Immunohistochemical staining showed that the cell-mediated contraction is associated with the α-smooth muscle actin phenotype of tendon cells *in vitro*. Strain imparted by cells in the sponges was nonuniform, with contraction occuring at the edges of the sponges first. This contraction was apparently due primarily to a cell continuous layer on the surface of the sponge. Histology of the sponges suggested that the cells within the pores of the sponges may also be exerting a force on the matrix.

It was determined that the cell-mediated contraction of CG sponges decreased with increasing apparent modulus of elasticity of the sponges.

Analysis of the sponge contraction among the various cross-linking groups showed that cell-mediated contraction is a function of the sponge modulus of elasticity, the cell type, including the α-smooth muscle actin phenotype, and the density and distribution of cells in the sponge.

4.1 Collagen Sponges

4.1.1 CG Sponges

The collagen-glycosaminoglycan (CG) sponges used for this research have been used succesfully in dermal [58] and peripheral nerve [9] wounds as scaffolds for regeneration. The CG sponges have primarily been implanted without the addition of exogenous cells. However, in avascular or poorly vascularized tissues which are sparsely populated with cells, the CG sponges alone may not be able to induce regeneration. As a result, investigators have researched the behavior of cells including chondrocytes [6], meniscus cells [40], and tendon fibroblasts [36] which had been seeded onto CG sponges. The goal of these studies was to determine if the CG sponges could successfully be seeded with cells for transplantation to a wound site. The porous architecture of the CG sponges encourages migration of cells from host tissue into which they are implanted, suggesting that seeded cells might also migrate easily into the porous sponges. Preliminary studies have shown that certain cell types will migrate into, attach to, and proliferate within the CG sponges [36, 40, 43]. These same studies have also noted that the CG sponges are contracted by exogenous cells, causing a reduction in the overall dimensions of the sponges, and in some cases, a curling up of the sponge edges. In addition, other researchers have noted the effect of cross-linking on the mechanical properties of CG sponges [12, 60]. Each of these factors contributed to the decision to use the CG sponges in this study of cell-mediated contraction of collagen sponges. While this thesis addressed the contraction of CG

sponges by cells *in vitro*, the knowledge gained may shed light on the contraction of unseeded implants by endogenous cells that infiltrate these sponges *in vivo*.

4.1.2 CG Sponge Synthesis

Synthesis of CG sponges resulted in 2-3 mm thick sheets of type I collagen-GAG sponges with randomly oriented pores. The pore diameter range was large (20 μm – 400 μm), with the average pore diameter being around 120 μm. This average pore diameter and range agreed closely with values obtained by other researchers synthesizing the same sponges. Areas which were noticeably thicker or thinner than the rest of the sponge were found in some of the sponges. The reason for the differences in these areas is unknown, and these areas were not used for either cell-seeding or mechanical testing.

Disks of CG sponge were cut from the sheets of sponges using a punch and hammer. At times, the cutting process seemed to compress the edges of the sponges. This compression appeared to be relieved by the rehydration of the sponges, and histological sections of the sponges showed no pore compression at the sponge periphery. The cutting process was difficult, however, requiring frequent re-sharpening of the punch. This re-sharpening of the punch was time consuming and difficult, and the extra handling of the instruments and sponges increases the chances of introducing infection.

An improved method for producing the sponges for seeding might involve the use of disk-shaped molds for freeze-drying so that the entire punching procedure can be eliminated.

4.1.3 Cross-linking of CG Sponges

Cross-linking of CG sponges was accomplished with both physical and chemical methods. Dehydrothermal (DHT) treatment is a physical cross-linking method which has been shown to increase the mechanical strength of biopolymers [57] and to prevent rapid degradation of these materials. All sponges were first DHT cross-linked for 24

hours following the normal laboratory protocol for CG sponge synthesis. CG sponges are generally not used without at least having been DHT cross-linked because they will rapidly degrade if they are not cross-linked. One group which was DHT cross-linked only was included in these experiments.

In earlier studies in which CG sponges were seeded with cells, sponges were soaked in 70% ethanol and rinsed with saline prior to seeding. The ethanol treatment was intended to sterilize the sponge for seeding. Differences in contraction of sponges which had been rinsed in ethanol and those which had only been rehydrated with saline [40] caused us to speculate that ethanol treatment was responsible for some degree of chemical cross-linking which caused the sponges to resist contraction. An ethanol treated group was included in this study in order to test this hypothesis. We found that ethanol treatment reduced cell-mediated contraction by approximately 50%.

Chemical cross-linking with glutaraldehyde had been described as a method for controlling degradation of the CG sponges [52, 60], and was also shown to affect the mechanical properties of CG sponges [12]. Glutaraldehyde, which is cytotoxic, is a problematic cross-linking agent for resorbable biomaterials, because the bound glutaraldehyde is released as the material degrades. For this study, however, glutaraldehyde was used to cross-link CG sponges because the degree of glutaraldehyde cross-linking and therefore, the mechanical properties of the sponges, can be easily controlled by varying the amount of time the sponges are exposed to the glutaraldehyde. CG sponges were cross-linked with glutaraldehyde for 30 minutes, 12 hours, and 24 hours in order to create sponges with varied stiffnesses. While the number of cells in the CG sponges treated with glutaraldehyde for 12 and 24 hours was less than the number in the specimens treated for 30 minutes, the results could not be attributed to a toxic effect of the aldehyde. Histology did not reveal noticeable cell death.

Exposure to ultraviolet irradiation (UV) is another physical cross-linking method which has been shown to alter the mechanical properties and degradation rate of collagen biomaterials [57], and UV cross-linking has been used in studies of cell-seeded

CG sponges [6, 40]. Physical methods of cross-linking such as DHT and UV avoid the problem of cytotoxic chemical cross-linking and are generally used as alternatives to chemical cross-linking. The degree of cross-linking of by UV irradiation is difficult to quantify because of factors which can vary, such as lamp intensity, specimen distance from the lamp, and thickness of the specimen. One group of UV irradiated sponges was included in this thesis. The protocol described by Nehrer, et al. [43] for UV cross-linking was used.

4.1.4 Type II Collagen Sponges

The type II collagen sponges were included in this study because they had been shown to resist contraction by chondrocytes *in vitro* [6, 43]. The type II sponges are noticeably stiffer than type I CG sponges when they are dry, and it was thought that this difference in stiffness may have been responsible for the difference in sponge contractability. The protocol for UV cross-linking and ethanol treatment of the type II sponges followed that of the studies in which no contraction of the type II sponges was seen.

4.2 Mechanical Testing

Tensile testing was performed on the collagen sponges to determine their moduli of elasticity. This testing was not meant to simulate or describe the contractile forces exerted by the cells on the sponges *in vitro*. Instead, the goal of the mechanical testing was to determine the stress-strain behavior of collagen sponges which were cross-linked to different degrees. A representative mechanical property of that behavior, the modulus of elasticity, would then be compared with the contraction of cell-seeded collagen sponges to determine if there was a relationship between the cell-mediated contraction and the modulus of elasticity of the sponges.

4.2.1 Testing Procedure

For each cross-linking group, at least two specimens were tested. The experimental design had called for at least three specimens to be tested for each group. However, on two occasions, a problem with the computer caused the force-time data to be lost, leaving the groups (12G and ETH) with data from only two tests. One of the tests for a UV cross-linked specimen was excluded from the study. The stress-strain curve for that specimen differed from the other UV cross-linked sponge. Review of the force-time data revealed that an error occurred as the data were being read or recorded, causing the force data to be artificially high. A 0.5G group specimen was damaged while being placed in the testing bath clamps and therefore not tested. Replacement specimens for the 12G and 0.5G groups were cross-linked at a later time and tested. The stress-strain curve for the 0.5G group was drastically different from those of the other two 0.5G specimens, which were very similar to each other. The third specimen failed at approximately 12% strain and a stress of 11 kPa, while the others reached strains nearer to 25% and stresses between 20 and 26 kPa. The data from the test of the third specimen were excluded because of these differences. The exclusion of this test was justified by the fact that the two specimens which behaved similarly were rehydrated and cross-linked at the same time, and the third specimen was cross-linked weeks later. The stress-strain curve for the 12G sponge which was cross-linked at a later time was also different than the other two specimens, but the differences were not as drastic as those seen in the 0.5G group, so the data from the third 12G sponge was included. Because the glutaraldehyde cross-linking process the used each time was not altered, these observations may indicate the variability inherent in the glutaraldehyde cross-linking method. This variability is unexplained, but must be taken into consideration in future work if glutaraldehyde cross-linking is to be used.

None of the type II collagen sponge mechanical test data were included in this thesis. The failure of the specimens at the clamped ends and the resulting stress-strain relationships appeared to be the result of the limitations of the specimens, which were smaller than the CG sponges and very fragile when rehydrated. It could

not be proved that these data did or did not represent the true stress-strain behavior of type II collagen sponges, so they were excluded.

In general, the apparatus used to perform the mechanical tests and to compute the strain seemed to provide consistent results. The computer errors which caused data from some tests to be lost were eventually determined to be operator-caused. Only in the case of the excluded UV cross-linked sponge test does it appear that the errors in force-time data were caused by a problem with the testing apparatus. The primary difficulty in using the testing bath involved clamping the sponge with the acrylic clamps. Although the design of the clamps seemed to prevent the sponges from failing at the clamps, it was often difficult to orient the sponge in the clamp properly, and on one occasion, the excessive handling of the specimen needed to place it in the clamp resulted in it being torn and rendered useless for testing. A redesign of the clamps to make them easier to use would improve the testing procedure and results.

4.2.2 Analysis of Mechanical Testing Data

The stress and strain data were computed and plotted as simple line graphs with lines connecting the consecutive data points. The shape of the lines plotted for all of the tests showed a concave up relationship between stress and strain, with the sponges stiffening as the strain increased. Because the curves were somewhat parabolic in shape, a second-order polynomial regression was performed on the stress and strain data set for each mechanical test rather than a simple linear regression.

The data very closely fit the curves which were calculated. The R^2 values for the curves ranged from 0.963 to 0.998. Because the coefficients of determination were so high, the curves and their equations were used to represent the mechanical properties of each sponge tested.

4.2.3 Modulus of Elasticity of CG Sponges

The modulus of elasticity for sponges from each treatment group increased with increasing strain. The stress-strain behavior of the uncross-linked and cross-linked groups was similar to that which had been noted in an earlier study [13], although the strains and stresses noted in that study were considerably higher, due to the difference in the CG sponges tested. Chen's study used a CG sponge "rod", a cylinder-shaped sponge with axially aligned pores with average diameters of 30 μm. The magnitudes of stress, strain, and modulus values calculated for this thesis are comparable to Chen's values when the differences in sponge geometry, pore diameter, and pore alignment are taken into account [30]. The average modulus for each treatment group was compared at 5, 10, and 15% strain (Figure 3-8). While half of the groups which were tested reached strains greater than 20%, the maximum strain used for this analysis was 15%, to account for the groups which failed at or around 15% strain.

At 5, 10, and 15% strain, the elastic modulus of DHT group sponges was significantly lower than that of all other groups which had been further cross-linked. Among the other groups at 15% strain, the difference in modulus of elasticity was significant only between the 24G and 0.5G groups. At 10% strain, differences in the elastic moduli were only significant between the ETH and 24G groups, and the 0.5G and 24G groups. Similar results were seen at 5% strain.

It is important to note that the mean elastic moduli which were not considered significantly different were not always close in value. An example of this can be seen in comparing the modulus values for the UV group and the 12G group at 15% strain (Table 3.1). The mean modulus value for the UV group is approximately 185 kPa, while the mean modulus value for the 12G group is approximately 138 kPa. Still, these values are not significantly different because of the large standard error associated with the low number of specimens tested. In the case of the DHT group, four specimens were tested, and all of the stress-strain curves were very similar to each other (Figure 3-1). As a result, the error for the DHT group values was relatively low. The 0.5G group mean modulus at all three strain values is an example of a case

in which the error is relatively low because the stress-strain curves were so similar (Figure 3-4). The 0.5G curves actually appear to be closer in shape and magnitude to each other at than the four DHT curves, but the standard error for the DHT group is lower because of the greater specimen number. In cases such as the UV group, however, in which the curves were similar but not as close as the DHT curves, the error is high. Assuming that additional specimens cross-linked in the same manner would also have similar stress-strain behavior, the error would be expected to decrease as more tests were included in the average. Thus, data from additional mechanical tests may show that the mean elastic moduli for most of the groups are significantly different from each other. Without that data, however, significant differences among most groups can only be found at 5% strain. The variability in mechanical properties of 0.5G and 12G specimens cross-linked at a later time is another reason for testing a greater number of specimens. Further mechanical testing on sponges from the various treatment groups is necessary to draw clear conclusions about the effect of each particular cross-linking method on the modulus of elasticity of the sponges.

4.3 Fibroblasts and Cell Seeding

4.3.1 Tendon Harvest and Digestion

Fibroblasts were harvested from calf patellar tendon within 3 hours of sacrifice, and the digestion of the tendon began within 5 hours of sacrifice. The length of time between animal sacrifice and the start of the collagenase digestion did not seem to have an adverse effect on the cell viability (85% viability), as 1.3 million live cells per gram of patellar tendon were obtained.

The process of digestion in trypsin and collagenase was used with this particular tissue because it has such low cell density. The process would allow for most of the cells to be released from the tendon extracellular matrix as it was digested by collagenase, providing a primary culture with a large number of cells. The drawback of the collagenase digestion is that it may affect the behavior of the cells, which must

survive lengthy periods of exposure to trypsin and collagenase.

Cells can also be obtained from the tissue through the use of explants. In this method, the tissue would be cut into small pieces, placed on a cell culture dish, and covered with culture medium. The cells then slowly migrate out of the tissue into the nutrient-rich atmosphere of the culture dish, attach to the dish, and begin to proliferate. This method avoids the effects of a lengthy enzymatic digestion. The outgrowth of cells from the tissue, however, is a slow process, and it is reasonable to believe that a percentage of the cells in the tissue will die before being able to migrate onto the medium-covered culture dish. In addition, the cells are still cultured on a two-dimensional culture dish as they are following digestion. This change in environment from three-dimensional collagen extracellular matrix to two-dimensional tissue culture dishes may also affect the phenotype of the cells.

Explants can also be placed directly on the sponge to be seeded, so that the cells can migrate directly into the sponges from the tissue. In studies where the behavior of a specific cell type from a specific source is to be studied while in the sponges, this method avoids both digestion and two-dimensional culture. The drawback of this method is that it is difficult to control the number of cells which are seeded in the sponge.

Tenocytes were used for this seeding experiment because tendon is one tissue for which cell-seeded CG sponges have been considered [37]. Additionally, the calf tendon was a readily available source. The collagenase digestion of the tendon tissue, while not ideal, allowed for retrieval of a large number of cells for culture, and did not appear to adversely affect the contractile nature of the tenocytes, and this was the behavior of the cells most important for this study.

4.3.2 Cell Seeding

Following the cross-linking and measurement of the sponges, the sponges were soaked in complete cell culture medium as the cells were being prepared for seeding. This step was intended to introduce the nutrients from the medium throughout the thickness of the sponge, thus providing an environment into which the cells would

migrate.

The "drying" step removed excess medium from the sponge, allowing the cell suspension room to infiltrate the sponge. This step improved the seeding of a highly concentrated suspension of cells in culture medium by preventing excessive spilling of the suspension off of the sponges and onto the culture wells.

Three percent of the cells which had been seeded onto the sponges remained in the medium after three days in culture. An assay of DNA content of the selected sponges after three days in culture showed that an average of 536,000 ± 156,000 cells in each sponge, and the original seeding density was 500,000 cells per sponge. The culture conditions and seeding method, therefore, appeared to have allowed for efficient seeding of fibroblasts into the sponges.

4.3.3 Cell Infiltration and Morphology

The infiltration of cells into the interior regions of the disk by the seventh day in culture showed that the fibroblasts were able to attach to and migrate within the sponges, although the majority of the cells were found in the edge regions of the disk at this time point. By the 14th and 21st day, cells had migrated throughout the sponges and proliferation was evident, both from histological sections and DNA assay. In sponges which underwent contraction (DHT, ETH, UV, and 0.5G), 10-30 μm thick layers of cells were present at the periphery of the disk at 14 and 21 days. In both the edge and center regions of these sponges, cells were both elongated and ovoid (Figure 3-10). In the CG sponges which underwent less contraction (12G and 24G), the cell layer at the sponge edges was present but not as thick. The cells in the interior of the disk were evenly distributed and fusiform in shape, elongated along the matrix fibers (Figure 3-11).

The difference in the distribution of the cells in the sponges is most likely due to the fact that the pores of the stiffer sponges were not as severely contracted by the cells, allowing for easier migration and infiltration. Even at 21 days, the pore structure of the 12- and 24-hour glutaraldehyde cross-linked sponges does not even appear to have been contracted by the cells. The open pores facilitate cell migration

throughout the sponge, resulting in a more even distribution of cells than is seen in the highly contracted sponges with closed pores. Another notable finding was that the DNA content, and thus the number of cells, in the DHT sponges was considerably lower than that of the ETH sponges. The ethanol treatment had originally been used as a method for sterilization and because earlier studies showed improved cell infiltration into ethanol-soaked sponges. This latter observation may be related to the modification of the wettability of the sponge by ethanol. The results of the DNA assay for this thesis support those studies.

The difference in cell morphology in sponges of different stiffnesses may be related to the contractile behavior of the cells in the sponge. In the stiffer sponge (Figure 3-11), all of the cells were highly elongated along the length of the open sponge pores at 21 days. In contrast, the sponges which underwent contraction (Figure 3-10) contained many more cells which are ovoid in shape at 21 days. This suggests that the elongated cells on stiffer sponges were exerting contractile forces on the pore walls, but that the stiffness of the sponge was high enough to resist the contractile force of the cells. The more ovoid shape of the cells in the lower modulus sponges may be related to the contracted state of the cells.

The contraction of the sponge pores is discussed in more detail in section 4.4.2.

4.4 Contraction of Collagen Sponges

4.4.1 Shrinkage and Cell-Mediated Contraction

Shrinkage of the sponges was noted in both the seeded and control sponges in several groups. The shrinkage of the unseeded control sponges is most likely explained by the presence of strains in the sponges following freeze-drying. The freeze-drying "sets" the sponge in a structure which then shrinks when the sponge is immersed in an aqueous medium because water is a mild plasticizer for collagen, and the strains are relieved [61]. Cross-linking the sponges can prevent this relaxation of the sponge strains, by chemically or physically "setting" the sponge structure. This is evident in

the lack of shrinkage of unseeded sponges which were cross-linked with glutaraldehyde and the slight shrinkage in the sponges cross-linked with ultraviolet irradiation.

In order to account for the shrinkage of the unseeded sponges, the cell-mediated contraction was defined as the percent contraction of the control sponges minus the percent contraction of the seeded sponges. The cell-mediated contraction was then divided by the average DNA content of the sponges in order to account for the number of cells in the sponges. In comparing the ETH and 0.5G groups at 21 days, the overall contraction in the ETH group is much greater than that of the 0.5G group (Figure 3-21). Computation of cell-mediated contraction shows that the results are not significantly different for these two groups. However, when the cell-mediated contraction is normalized by the mean DNA content in the sponges, the difference between the 0.5G and ETH group contraction becomes evident (Figure 3-27).

The calculation of cell-mediated contraction and the normalization of that value by the DNA content resulted in a relationship between contraction and cross-linking groups that closely matched what was expected based on the results of other studies and on previous experience. Because the type I CG sponges were all initially DHT cross-linked, it was expected that the sponges which were not cross-linked any further (DHT) would undergo the most cell-mediated contraction. The glutaraldehyde cross-linked sponges were expected to contract less as their cross-linking time increased, and this relationship is evident in Figure 3-27. The contractability of the ethanol and UV cross-linked groups were expected to fall between the DHT group and the glutaraldehyde treated groups.

Based on an earlier study [43], the type II collagen sponges were not expected to contract. The unseeded control sponges were smaller than the seeded type II collagen sponges, resulting in the negative contraction values shown in Figure 3-27. The reason for this is unexplained, however, the results still show that the type II sponges are not contracted by the seeded fibroblasts. It is worth noting that the type II sponges had the greatest DNA content, and upon rehydration, became very fragile. Still, these densely populated, low modulus sponges underwent no contraction. This result is evidence that cells' inability to contract these sponges may be related to factors other

than the sponge stiffness, including biochemical composition of the sponges.

4.4.2 Contraction of Pores

The contraction of the pores in the sponges was investigated with the light microscope. Clear differences can be seen in the pores of an ethanol (ETH) treated sponge at 21 days, and a 24G sponge at 21 days (Figure 3-25). In the sponges which were greatly contracted, micrographs of the sponges at the different time periods Figures 3-23 – 3-24) showed that the contraction of the pores was nonuniform, occurring in the edge region of the disk first. By the 14th day in culture, the pores at the edge of the disk were almost completely closed, but the pores in the center of the disk were still somewhat open. Hematoxylin and eosin-stained sections highlight a multilayered cell capsule at the periphery of the sponge. In addition, there were many more cells visible in the edge region of the sponges than in the center at all time points. This cell continuous layer at the periphery is most likely responsible for contracting the edge region of the sponge during the earlier time periods. At the same time that the cells in the edge are contracting the matrix pores, the cells inside the sponges are proliferating and beginning to exert more significant contractile forces directly on the walls of the scaffold to contract the inner pores.

4.4.3 Presence and Role of Myofibroblasts

Because myofibroblasts have been implicated in the contraction of biomaterials such as collagen lattices and gels [4], as well as the CG sponges [6, 36, 40, 43], their role in the cell-mediated contraction of the cross-linked CG sponges in this study was investigated. The immunohistochemical stain for α-smooth muscle actin clearly demonstrated the presence of this contractile actin isoform in the cytoplasm of a large majority of cells in the scaffolds from all cross-linking groups and all time periods. Cells were stained positive for α-smooth muscle actin in almost equal percentages in the edge and center regions of the sponges, with almost all of the cells in both regions staining positively, and all of the cells in the multi-layered cell capsule at the periphery

staining positively. At no time period or sponge region was a high percentage of cells noted that did not stain positively for α-smooth muscle actin. These findings suggest that the contraction of the sponges is the result of myofibroblast activity. It is worth noting that the cells used for this work may have expressed the myofibroblast phenotype while still in 2-D culture. Investigators have found the α-smooth muscle actin isoform in varying percentages in corneal fibroblasts attached to tissue culture wells [39], therefore it is possible that some percentage of the cells used for this work expressed the myofibroblast phenotype prior to seeding.

Investigators have proposed that cell contraction of biomaterials is the result of contractile forces generated by myofibroblasts, while others have concluded that the contractile force is provided by migrating fibroblasts [22, 23]. The immunohistochemical stain used to analyze sections of the sponges for this study clearly shows a high percentage of myofibroblasts in the matrix. This suggests that myofibroblast contraction is responsible for the contraction of the sponges. It is notable, however, that the contraction of these sponges was first seen in the edge regions, which were densely populated by myofibroblasts even at early time points, and which were surrounded by a cell-continuous layer. The center region contained myofibroblasts at early time periods as well, although the density of both myofibroblasts and fibroblasts in the interior of the sponge was much lower than in the edge region. It is reasonable to believe that at early time points, cells were migrating from the edge regions of the sponges into the center region. Because most of the cells in the edge region were myofibroblasts, it would appear that the cells migrating into the sponge interior were myofibroblasts. Therefore, it may be that the contraction of the sponge pores was the result of a combination of simple myofibroblast contraction by the cells at the periphery and edge region of the sponge, as well as by myofibroblast locomotive forces as they migrated into the interior of the sponge. A combination of contractile and locomotive forces, therefore, may be responsible for the highly contracted pores in the sponge edge regions at earlier time points, and for the contracted pores throughout the sponges at later time points.

4.5 Effect of Modulus of Elasticity on Cell-Mediated Contraction

The effect of modulus of elasticity on cell-mediated contraction was determined by plotting the normalized average cell-mediated contraction at 21 days against the average moduli of elasticity at 10 and 15% strain. Based on the linear regression model of the effect of modulus of elasticity on cell-mediated contraction, a modulus value could be chosen which would allow only a desired amount of contraction of the sponges. An appropriate method could then be chosen to cross-link the sponges to obtain the needed elastic modulus.

Chapter 5

Conclusions

Tendon fibroblasts will attach to, migrate into, and proliferate within CG sponges. A large majority of cells seeded in CG sponges express the myofibroblast phenotype. These cells are able to contract sponges with low stiffness, but their contractile force is not sufficient to contract the stiffer sponges used in this study.

There is a relationship between the cell-mediated contraction of CG matrices and modulus of elasticity. From this relationship, DHT treatment alone is not sufficient to resist contraction by tendon fibroblasts seeded at the density used in this experiment. The distribution of cells and the nonuniformity of contraction in the sponges varies with cross-linking treatment. These factors need to be considered, along with modulus of elasticity, in treatment of matrices to achieve selected contraction resistance. In this regard, the mean modulus for CG sponges may have to be tripled from the DHT level in order to resist contraction.

The similarity in modulus values for the ETH, UV, and 0.5G groups, and the comparable cell-mediated contraction indicates that physical cross-linking methods such as UV irradiation can be effectively used to control the elastic modulus and as a result, the cell-mediated contraction of the sponges. Use of physical cross-linking methods may improve cell viability in the sponges because the potentially cytotoxic chemicals most often used for cross-linking can be avoided.

Chapter 6

Future Work

6.1 Mechanical Testing of CG Sponges

Further tensile testing of CG sponges with a higher sample number should be done to reduce error. In addtion, improvements in the design of the testing apparatus may make the testing procedure easier and less likely to cause specimen damage. Tensile tests of the type II sponges should also be attempted using a different specimen size or shape to prevent the problems encountered in this experiment. The effect of strain rate on the stress-strain behavior of CG sponges should also be studied.

Because cells attached to the sponges are exerting a compressive force on the pore walls, compression testing of CG sponges may provide valuable insight into the sponge stiffness needed to resist contraction.

6.2 Cross-Linking Treatment

Cross-linking treatments should be replicated in several batch processes in order to determine the reproducibility of the methods. Ultraviolet irradiation of sponges should be improved so that cross-linking of sponges is more uniform. Additionally, cross-linking of sponges with UV and DHT for various times should be done in order to determine the suitability of these methods for producing sponges of varying stiffnesses.

6.3 Cells and Cell-Seeding

Study of additional cell types seeded into the sponges should be done to determine the extent to which cell type determines the degree of sponge contraction. In addition to varying cell type, the number of cells seeded into the sponges and the cell passage number should also be varied to determine the effects of those factors.

Transmission electron microscopy should be used to provide ultrastructural evidence of the myofibroblast phenotype in cells attached to the CG sponges.

6.4 Cell-Mediated Contraction of Collagen Sponges

The present findings have provided a useful guide for the cross-linking treatment of CG matrices relative to cell-mediated contraction. Future work should quantify the nonuniform pore deformation with time, and explore the relationship between matrix contraction and certain compressive properties to obtain a more accurate model.

Appendix A

MATLAB Code for Disk Measurement

```
function y=process(file_list,dime_file)

% Process image files, processed image output to $file.prc, area
% information output to $file.info.  info file contains pixel count,
% area, and the name of the dime file used to calculate area.
%
% Input to the function is the list if files and the name of the dime file.
%  process('(file list)','(dime file)');

%%%% Process dime image %%%%

dime_jpg=imread(num2str(dime_file)); % Read in dime image
dime_jpg=double(dime_jpg);           % Convert image data to double floats
dime_img=sqrt(dime_jpg(:,:,1).^2+dime_jpg(:,:,2).^2+dime_jpg(:,:,3).^2); "Energy"
dime_img=dime_img-min(min(dime_img)); % Normalize "energy" values to [0,1]
dime_img=dime_img/max(max(dime_img)); %              "
dime_img=dime_img<.5;                 % Background/Dime decision
dime_img(:,1)=zeros(240,1);          % Get rid of bad edges from
dime_img(236:240,:)=zeros(5,360);    % video capture
dime_area_pix=sum(sum(dime_img));    % Area of dime in pixels
dime_area_sq_mm=249.9652;            % Area of dime in sq. mm.
```

```
%%%% Process files in file list %%%%

garb=strcat('fid=fopen('' ',num2str(file_list),''','''rt''');');
eval(garb);
while 1
  file = fgetl(fid);             % Load file name
  if ~isstr(file), break, end
  fprintf('%s\n',num2str(file))
  file_prefix=strtok(file,'.');  % remove file suffix
  prc_file=strcat('/home/dst/Contraction_Images/',num2str(file_prefix),'.prc');
  dat_file=strcat('/home/dst/Contraction_Images/',num2str(file_prefix),'.dat');

  file_jpg=imread(num2str(file));  % Read Image
  file_jpg=double(file_jpg);       % Convert image data to double floats
  file_img=sqrt(file_jpg(:,:,1).^2+file_jpg(:,:,2).^2+file_jpg(:,:,3).^2); % "Energy"
  file_img=file_img-min(min(file_img));  % Normalize "energy" values to [0,1]
  file_img=file_img/max(max(file_img));  %   ""
  file_img=file_img<.5;                  % Background/Disk decision
  file_img(:,1)=zeros(240,1);            % Get rid of bad edges from video capture
  file_img(236:240,:)=zeros(5,360);      %              ""
  imwrite(file_img,num2str(prc_file),'jpg'); % Save processed file
  fid2=fopen(num2str(dat_file),'w');
  file_area_pix=sum(sum(file_img));      % Calculate area in terms of pixels
  fprintf(fid2,'%s %g %d\n',num2str(dime_file),\
  file_area_pix/dime_area_pix*dime_area_sq_mm,file_area_pix);   % Write data to file
  fclose(fid2);
end
fclose(fid);
y=1;
```

Bibliography

[1] A. A. Amis, J. R. Campbell, S. A. Kempson, and J. H. Miller. Comparison of the structure of neotendons induced by implantation of carbon or polyester fibres. *Journal of Bone and Joint Surgery*, 66-B:131–139, 1984.

[2] P. Arora and C. M^{c}Culloch. Dependence of collagen remodelling on alpha-smooth muscle actin expression by fibroblasts. *J. Cell. Physiol.*, 159:161–175, 1994.

[3] E. Bell, B. Ivarsson, and C. Merrill. Production of a tissue-like structure by contraction of collagen lattices by human fibroblasts of different proliferative potential in vitro. In *Proc. Natl. Acad. Sci*, volume 76, pages 1274–1278, USA, 1979.

[4] C. Bellows, A. Melcher, and J. Aubin. Fibroblasts contracting three dimensional collagen gels exhibit ultrastructure consistent with either contraction or protein secretion. *J. Ultrastructure Res.*, 78:178–192, 1982.

[5] M. M. Belmonte, G. Biagini, G. Ricotti, C. Zucchini, C. Castaldini, M. Fini, R. Giardino, and M. Bigini. Experimental wound dressing by heterologous collagen – a morphological–quantitative approach. *Journal of Bioactive and Compatible Polymers*, 8(4):365–382, October 1993.

[6] H. A. Breinan. *Development of a Collagen-Glycosaminoglycan Analog of Extracellular Matrix to Facilitate Articular Cartilage Regeneration.* PhD thesis, Massachusetts Institute of Technology, 1998.

[7] J. F. Burke, I. V. Yannas, W. C. Quinby, C. C. Bondoc C. C., and W. K. Jung.

Successful use of a physiologically acceptable artificial skin in the treatment of extensive burn injury. *Ann. Surg.*, 194:413–428, 1981.

[8] Y. Cao, J. P. Vacanti, X. Ma, K. T. Paige, J. Upton, Z. Chowanski, B. Schloo, R. Langer, and C.A C. A. Vacanti. Generation of neo-tendon using synthetic polymers seeded with tenocytes. *Transplant Proc.*, 26(6):3390–3391, 1994.

[9] L. J. Chamberlain. Long term functional and morphological evaluation of peripheral nerves regenerated through degradable collagen implants. Master's thesis, Massachusetts Institute of Technology, 1996.

[10] L. J. Chamberlain and I. V. Yannas. Methods for the preparation of collagen-glycosaminoglycan copolymers for tissue regeneration. In J. Morgan and M. Yarmush, editors, *Methods for Tissue Engineering.* Humana Press, 1998.

[11] A.S.-P Chang. Electrophysiological recovery of peripheral nerve regenerated by biodegradable polymer matrix. Master's thesis, Massachusetts Institute of Technology, 1988.

[12] C. Chen, I. V. Yannas, and M. Spector. Pore strain behaviour of collagen-glycosaminoglycan analogues of extracellular matrix. *Biomaterials*, 16:777–783, 1995.

[13] C. S. Chen. Design and analysis of a cell culture system that uses a three-dimensional tissue analog to investigate the role of mechanical forces in connective tissue maintenance. Master's thesis, Massachusetts Institute of Technology, 1993.

[14] D. R. Cooper and R. J. Davidson. The effect of ultraviolet irradiation on soluble collagen. *Biochem. J.*, 97:139–143, 1965.

[15] L. Dahners, A. Banes, and K. Burridge. The relationship of actin to ligament contraction. *Clin. Orthop. Relat. Res.*, 210:246–251, 1986.

[16] I. Darby, O. Skalli, and G. Gabbiani. Alpha-smooth muscle actin is transiently expressed during experimental wound healing. *Lab. Invest.*, 63:21–29, 1990.

[17] P. A. Davis, S. J. Huang, L. Ambrosio, D. Ronca, and L. Nicolais. A biodegradable composite artificial tendon. *Journal of Materials Science: Materials in Medicine*, 3:359–364, 1992.

[18] C. J. Doillon, F. H. Silver, and R. A. Berg. Fibroblast growth on a porous collagen sponge containing hyaluronic acid and fibronectin. *Biomaterials*, 8:195–200, 1987.

[19] C. J. Doillon, A. J. Wasserman, R. A. Berg, and F. H. Silver. Behaviour of fibroblasts and epidermal cells cultivated on analogues of extracellular matrix. *Biomaterials*, 9:91–96, 1988.

[20] G. A. Dunn and J. P. Heath. A new hypothesis of contact guidance in tissue cells. *Exp. Cell Research*, 101:1–14, 1976.

[21] M. G. Dunn, J. B. Liesch, M. L. Tiku, and J. P. Zawadsky. Development of fibroblast-seeded ligament analogs for acl reconstruction. *Journal of Biomedical Materials Research*, 29:1363–1371, 1995.

[22] H. Ehrlich and J. Rajaratnam. Cell locomotion forces versus cell contraction forces for collagen lattice contraction: An in vitro model of wound contraction. *Tissue Cell*, 22:407–417, 1990.

[23] H. P. Ehrlich. Wound closure: Evidence of cooperation between fibroblasts and collagen matrix. *Eye*, 2:149–157, 1988.

[24] O. S. Ejim, G. W. Blunn, and R. A. Brown. Production of artificial-oriented mats and strands from plasma fibronectin: a morphological study. *Biomaterials*, 14:743–748, 1993.

[25] D. L. Ellis and I. V. Yannas. Recent advances in tissue synthesis in vivo by use of collagen-glycosaminoglycan copolymers. *Biomaterials*, 17:291–299, 1996.

[26] J. Estes, J. Vande Berg, N. Adzick, T. MacGillivray, A. Desmouliere, and G. Gabbiani. Phenotypic and functional features of myofibroblasts in sheep fetal wounds. *Differentiation*, 56:173–181, 1994.

[27] D. Faryniarz, C. Chaponnier, G. Gabbiani, I. Yannas, and M. Spector. Myofibroblasts in the healing lapine medial collateral ligament: Possible mechanisms of contraction. *J. of Orthop. Res.*, 14:228–237, 1996.

[28] T. Finesmith, K. Broadley, and J. Davidson. Fibroblasts from wounds of different stages of repair vary in their ability to contract a collegen gel in response to growth factors. *J. Cell. Physiol.*, 144:99–107, 1990.

[29] T. Freyman. Specifications for tensile testing of collagen-gag matrices. Unpublished protocol.

[30] T. Freyman. Personal communication, 1998.

[31] G. Gabbiani, G. Ryan, and G. Majno. Presence of modified fibroblasts in granulation tissue and their possible role in wound contraction. *Experentia*, 27:549–550, 1971.

[32] A. K. Harris. Tissue culture cells on deformable substrata: biomechanical implications. *J. Biomech. Eng.*, 106(1):19–24, Feb. 1984.

[33] E. Ippolito, P. Natali, F. Postacchini, L. Accinni, and C. De Martino. Ultrastructural and immunochemical evidence of actin in the tendon cells. *Clin. Orthop. Relat. Res.*, 126:282–284, 1977.

[34] Y. Kato and F. Silver. Formation of continuous collagen fibers: Evaluation of biocompatibility and mechanical properties. *Biomaterials*, 11:169–175, 1990.

[35] Y. P. Kato, M. G. Dunn, J. P. Zawadsky, A. J. Tria, and F. H. Silver. Regeneration of achilles tendon with a collagen tendon prosthesis: Results of a one-year implantation study. *Journal of Bone and Joint Surgery*, 73-A(4):561–574, 1991.

[36] L. Louie, D. Schulz-Torres, L. Sullivan, I. V. Yannas, and M. Spector. Behavior of fibroblasts cultured in collagen-gag copolymer matrices. In *Transactions of the Society for Biomaterials*, page 25, 23rd Annual Meeting, New Orleans, 1997.

[37] L. K. Louie. *Effect of a Porous Collagen-Glycosaminoglycan Copolymer on Early Tendon Healing in a Novel Animal Model.* PhD thesis, Massachusetts Institute of Technology, 1997.

[38] L. K. Louie, I. V. Yannas, H. P. Hsu, and M. Spector. Healing of tendon defects implanted with a porous collagen-gag matrix: Histological evaluation. *Tissue Engineering*, 3(2):187–195, 1997.

[39] S. K. Masur, H. S. Dewal, T. T. Dinh, I. Erenburg, and S. Petridou. Myofibroblasts differentiate from fibroblasts when plated at low density. *Proc. Natl. Acad. Sci. USA*, 93:4219–4223, April 1996.

[40] S. M. Mueller, H. A. Breinan, S. Shortkroff, T. O. Schneider, and M. Spector. Alpha-smooth muscle actin in bovine meniscus cells seeded in type I and type II collagen-gag matrices. In *Transactions of the 44th Annual Meeting of the Orthopedic Research Society.* Orthopedic Research Society, 1998.

[41] P. K. Narotam, J. R. Vandellen, and K. D. Bhoola. A clinicopathological study of collagen sponge as a dual graft in neurosurgery. *Journal of Neurosurgery*, 82(3):406–412, March 1995.

[42] T. Nastume, O. Ike, T. Okada, N. Takimoto, Y. Shimizu, and Y. Ikada. Porous collagen sponge for esophageal replacement. *Journal of Biomedical Materials Research*, 27(7):867–875, July 1993.

[43] S. N. Nehrer, H. A. Breinan, A. Ramappa, G. Young, S. Shortkroff, L. K. Louie, C. B. Sledge, I. V. Yannas, and M. Spector. Matrix collagen type and pore size influence behavior of seeded canine chondrocytes. *Biomaterials*, 18:769–776, 1997.

[44] M. Nevins, C. KirkerHead, M. Nevins, J. A. Wozney, and R. Palmer. Bone formation in the goat maxillary sinus induced by absorbable collagen sponge implants impregnated with recombinant human bone morphogenetic protein-2. *International Journal of Periodontics and Restorative Dentistry*, 16:9–19, 1996.

[45] D. P. Orgill. *The Effects of an Artificial Skin on Scarring and Contraction in Open Wounds.* PhD thesis, Massachusetts Institute of Technology, 1983.

[46] F. Postacchini, P. Natali, L. Accinni, E. Ippolito, and C. De Martino. Contractile filaments in cells of regenerating tendon. *Experimentia*, 33:957–959, 1977.

[47] G. Ryan, W. Cliff, G. Gabbiani, C. Irle, D. Montandon, P. Statkov, and G. Majno. Myofibroblasts in human granulation tissue. *Human Pathol.*, 55(5), 1974.

[48] S.-J. Shieh, M. C. Zimmerman, and J. R. Parsons. Preliminary characterization of bioresorbable and nonresorbable synthetic fibers for the repair of soft tissue injuries. *Journal of Biomedical Materials Research*, 24:789–808, 1990.

[49] O. Skalli, P. Ropraz, A. Trzeciak, G. Benzonana, D. Gillessen, and G. Gabbiani. A monoclonal antibody against alpha-smooth muscle actin: A new probe for smooth muscle differentiation. *J. Cell Biol.*, 103:2787–2796, 1986.

[50] R. Stern, M. McPherson, and M. T. Longaker. Histologic study of artificial skin used in the treatment of full-thickness thermal injury. *J Burn Care Rehabil.*, 11:7–13, 1990.

[51] K. R. Stone, W. R. Rodkey, R. J. Webber, L. McKinney, and J. R. Steadman. Future directions: Collagen-based prostheses for meniscal regeneration. *Clinical Orthopaedic and Related Research*, 252:129–135, 1990.

[52] K. S. Troxel. *Delay of Skin Wound Contraction by Porous Collagen-GAG Matrices.* PhD thesis, Massachusetts Institute of Technology, 1994.

[53] T-L. Tuan, A. Song, S. Chang, S. Younai, and M. Nimni. In vitro fibroplasia: Matrix contraction, cell growth, and collagen production of fibroblasts cultured in fibrin gels. *Exper. Cell Res.*, 223:127–134, 1996.

[54] C. Vacanti, W. Kim, J. Upton, G. Schloo, and J. Vacanti. Tissue engineered composites of bone and cartilage using synthetic polymers seeded with two cell types. *Proc. 39th ORS Meeting*, page 276, San Fransisco, 1993.

[55] P. B. van Wachem, M. J. A. van Luyn, and M. L. Ponte da Costa. Myoblast seeding in a collagen matrix evaluated in vitro. *J Biomed. Mater. Res.*, 30:353–360, 1996.

[56] H. L. Wald, G. Sarakinos, M. D. Lyman, A. G. Mikos, J. P. Vacanti, and R. Langer. Cell seeding in porous transplantation devices. *Biomaterials*, 14(4):270–278, 1993.

[57] K. S. Weadock, E. J. Miller, L. D. Bellincampi, J. P. Zawadsky, and M. G. Dunn. Physical crosslinking of collagen fibers: Comparison of ultraviolet irradiation and dehydrothermal treatment. *J Biomed. Mater. Res.*, 29:1373–1379, 1995.

[58] I. V. Yannas. Regeneration of skin and nerve by use of collagen templates. In M. E. Nimmi, editor, *Collagen: Volume III, Biotechnology*, pages 87–115. CRC Press, Inc., Boca Raton, FL, 1988.

[59] I. V. Yannas. Certain biological implications of mammalian skin regeneration by a model extracellular matrix. In G. Abatangelo and J. M. Davidson, editors, *Cutaneous Development, Aging and Repair*, volume 18 of *Fidia Research*, pages 131–139. Liviana Press, Padavo, 1989.

[60] I. V. Yannas, J. F. Burke, P. L. Gordon, C. Huang, and R. H. Rubenstein. Design of an artificial skin. II. control of chemical composition. *J Biomed. Mater. Res.*, 14:107–131, 1980.

[61] I.V. Yannas. Personal communication, 1998.